Available online at www.sciencedirect.com
SCIENCE DIRECT®
Precambrian Research 132 (2004) 179–206
Precambrian Research
www.elsevier.com/locate/precamres

Characteristics and geochemistry of Precambrian ophiolites and related volcanics from the Istanbul–Zonguldak Unit, Northwestern Anatolia, Turkey: following the missing chain of the Precambrian South European suture zone to the east

Erdinç Yiğitbaş [a,*], Robert Kerrich [b], Yücel Yılmaz [c], Ali Elmas [d], Qianli Xie [b]

[a] Department of Geology, Faculty of Engineering and Architecture, Canakkale Onsekiz Mart University, Terzioglu Campus, TR 17020, Canakkale, Turkey
[b] Department of Geological Sciences, The University of Saskatchewan, Saskatchewan, Sask., Canada S7N 5E2
[c] Kadir Has University, Cibali, TR 34320, Istanbul, Turkey
[d] Department of Geology, Engineering Faculty, The University of İstanbul, Avcılar, TR 34850, Istanbul, Turkey

Received 21 May 2003; accepted 10 March 2004

Abstract

The Precambrian metamorphic basement of the Istanbul–Zonguldak Unit (IZU), NW Anatolia, Turkey, is represented by the Sünnice Group, composed essentially of four different metamorphic assemblages: (1) Çele metaophiolite, (2) Yellice metavolcanics, (3) Demirci metamorphics, and (4) Dirgine metagranite. The field relations and structural characteristics of these units were studied and representative geochemical analyses of Çele metaophiolite and related volcanics were obtained from the Sünnice, Almacık, and Armutlu areas. Collectively, the results are interpreted as the Çele Magmatic suite displaying disrupted components of a complete suprasubduction ophiolite. The Yellice metavolcanic sequence contains fragments of both an intra oceanic island arc and a back-arc basin association built on the ophiolite. The Demirci metamorphics represent reworked continental fragments forming the base of the metamorphic massifs. These three different metamorphic units were intruded, after their amalgamation, by the Dirgine granitic pluton dated at 570–590 Ma [Geol. Mag. 136 (5) (1999) 579; Int. J. Earth Sci. (Geol. Rundsch) 91 (3) (2002) 469]. The metamorphic tectonic units and the metagranite are collectively overlain by a thick Lower Ordovician to Carboniferous sedimentary cover known as the Istanbul–Zonguldak succession. The collisional event which led to the amalgamation of the different tectonic entities is partly penecontemporaneous with the Pan-African orogeny supporting the view that the basement of the IZU formed a link between the Pan-African and Trans-European suture zones.

Keywords: Turkey; Precambrian; Ophiolite; Oceanic island-arc; Geochemistry; Geotectonics

1. Introduction and scope

In terms of geodynamic significance, metamorphic basement associations within orogenic belts have often posed a geological enigma, particularly old basement tectonically incorporated into younger orogenic belts. Metamorphic basement associations exposed within Tethyan realms are no exception, representing fragments of tectonostratigraphic terranes of different age ranges, representing distinct geodynamic environments.

* Corresponding author. Fax: +90-286-2180541.
E-mail address: eyigitbas@comu.edu.tr (E. Yiğitbaş).

0301-9268/$ – see front matter © 2004 Elsevier B.V. All rights reserved.
doi:10.1016/j.precamres.2004.03.003

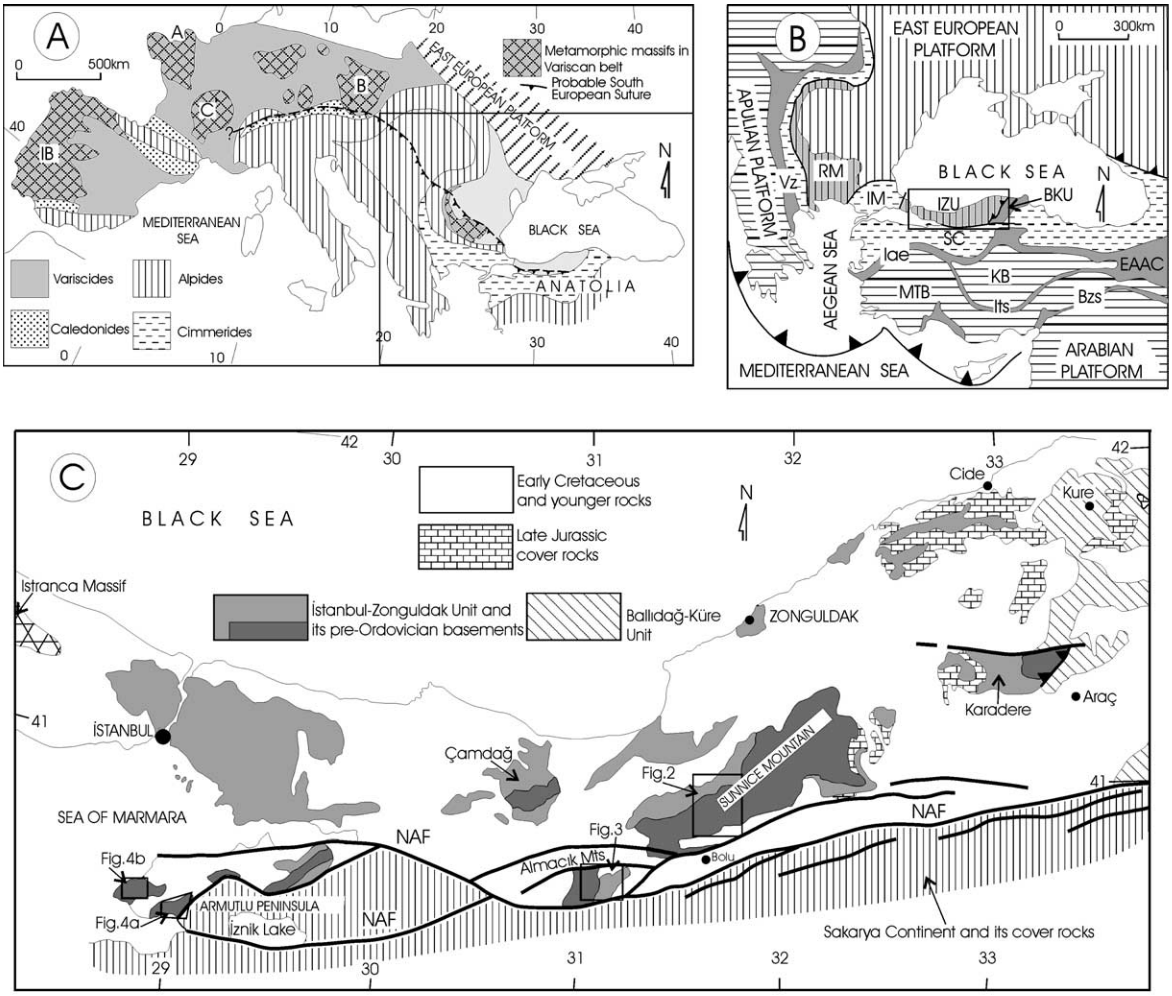

Fig. 1. (A) Generalized geotectonic map illustrating the position of the Turkish orogenic collage in the framework of the main tectonic divisions of Europe (European part of the map after Goodwin, 1991; Haydoutov, 1995). The European massifs including the Precambrian ophiolitic assemblages shown as capital letters: IB, Iberian; A, Armorican; C, Central; B, Bohemian. Quadrangle inset indicates the location of (B). (B) Major Cimmerid and Alpid tectonic division of Anatolia, Turkey and part of Balkan region (modified after Şengör, 1984). Tectonic elements originating in Gondwana are shown as horizontal, whereas those of the Laurasian are vertical ruling. Cimmeride fragment is shown as discontinuous horizontal lines. Remnants of the Neo-Tethyan sutures are: Iae, Izmir–Ankara–Erzincan Suture; Its, Inner-Tauride Suture; Vz, Vardar Zone; Bzs, Bitlis-Zagros Suture. Continental fragments are: KB, Kırşehir Block; MTB, Menderes–Taurus Block; IZU, Istanbul–Zonguldak Unit; SC, Sakarya Continent; RM, Rhodope Massif; BKU, Ballıdağ–Küre Unit. Paleo-Tethyan sutures shown as bold lines and triangles indicate subduction polarity where it is known. Quadrangle indicates the location of (C). (C) Outcrop pattern of the Istanbul–Zonguldak Unit and related assemblages. Insets show the location of the maps displayed in the corresponding figures.

The Northwestern Anatolian basement is a typical example (Fig. 1). The origin and primary geodynamic setting of old metamorphic basement associations remain unconstrained, with many different hypotheses offered for their origins, based on reconnaissance mapping and preliminary petrological studies (Kaya, 1977; Göncüoğlu et al., 1987; Göncüoğlu, 1997; Yılmaz et al., 1994; Yiğitbaş and Elmas, 1997; Yiğitbaş et al., 1995, 1999; Ustaömer, 1999; Ustaömer and Rogers, 1999; Chen et al., 2002) (Table 1).

In order to determine the major magmatic rock types, and constrain their original geodynamic

Table 1
Summary of the characteristics of Sunnice tectonostratigraphic terrane

Region	Reference	Basement	Cover	Interpretation
Almacık mountain	Abdüsselamoğlu (1959)	*Crystalline basement*: gneiss, amphibolite, schist	Devonian sedimentary sequence	Pre-Devonian metamorphic basement
	Yılmaz et al. (1981)	*Almacık Ophiolite*: Ordered ophiolite–Upper Cretaceous	Metamorphosed equivalent of İstanbul–Zonguldak Paleozoic sequence	İstanbul–Zonguldak Paleozoic sequence thrusted over Upper Cretaceous ophiolite
Armutlu peninsula	Kaya (1977)	*Precambrian–pre-Ordovician*: (1) ultramafic complex, (2) amphibolite-banded gneiss unit, (3) Fındıklı metavolcanics–metaclastics, (4) Orhangazi marble	Ordovician–pre-Permian: (1) Tazdağ quartz-arenite unit, (2) Kapaklı sublitarenite unit, (3) Kayalı limestone, (4) Cihatlı limestone	Silicic basement in the north and mafic one in the south of Büyük Kumla–Akçat tectonic divide, respectively
	Kaya and Kozur (1987)	*Pre-Jurassic basement*: (1) ultramafic tectonite unit, (2) amphibolite-banded gneiss unit	*Pre-Jurassic cover*: (1) Orhangazi Marble, (2) Fındıklı Formation	Different basement rocks organized structurally during pre-Jurassic period
	Göncüoğlu et al. (1987), Göncüoğlu (1997)	*Pamukova metamorphics*: Precambrian: metagranite, amphibolite, quartzite, marble	*Pamukova metamorphics*: early Paleozoic: metaclastics, recrystallized limestone, metasiltstone, shale	The basement complex has common features with the Precambrian ophiolites and island arc associations of the Balkan terrane
	Yılmaz et al. (1990, 1994, 1997)	*Armutlu metamorphic association*: amphibolite, metagabbro, hornblend schist, metabasite, leuco-granite	Metamorphosed equivalent of İstanbul–Zonguldak Paleozoic sequence	A pre-Paleozoic ophiolite of unknown origin
Sünnice mountain	Cerit (1990)	*Pre-Ordovician basement*: (1) Sünnice Group: high grade metamorphic basement, (2) Yellice Formation: Ordovician metavolcanic association, (3) Bolu Granitoids	Ordovician to Devonian Paleozoic sequence	(1) Continental basement, (2) Ensialic volcanic arc, (3) S-type granites
	Ustaömer (1999), Ustaömer and Rogers (1999)	*Pre-early Ordovician basement*: (1) Sünnice Group: migmatitic assemblages, (2) Bolu Granitoid Complex, (3) Çaşurtepe Formation: volcanic, volcaniclastic sequence	Işığandere Formation: basement lithology of the Paleozoic succession	Cadomian active continental setting: (1) a continental fragment, (2) pre-early Ordovician Cadomian arc-type Granitoid, (3) subduction-related volcanic sequence
	Yiğitbaş and Elmas (1997), Yiğitbaş et al. (1999)	*Pre-early Ordovician basement*: (1) Demirci metamorphics: high grade schists and migmatites, (2) Çele metaophiolites: Ordered ophiolites, (3) Yellice metavolcanics: volcanic, volcaniclastic suite, (4) Granitic assemblages	Metamorphosed equivalent of İstanbul–Zonguldak Paleozoic sequence	Pre-early Ordovician orogenic mosaic: (1) a continental fragment, (2) oceanic fragments, (3) intraoceanic island arc, (4) composite granites of different ages and tectonic settings

setting, we have undertaken a field-based project in Northwestern Anatolia to test previous hypotheses. A summary of the main field results from detailed geological mapping over a region of 3000 km^2 completed over 7 years is documented here. High precision trace element data are reported on subsets of the major rock types to constrain their original geodynamic environment.

2. Geological setting

Some of the Northwestern Anatolian metamorphic basement associations, which are covered by early Paleozoic units (i.e. Karadere, Sünnice, Almacık, Çamdağ and Armutlu massifs; Fig. 1C), were previously regarded as the oldest in Turkey, being Precambrian in age, without paleontologic and/or radiometric age data (Arpat et al., 1978; Kaya, 1977; Göncüoğlu et al., 1987; Göncüoğlu, 1997; Yılmaz et al., 1997). A Precambrian age was subsequently confirmed based on radiometric dating (Ustaömer and Rogers, 1999; Chen et al., 2002; Ustaömer et al., 2003). Within these basement associations, ophiolitic fragments were first recorded in the Almacık Mountains and Armutlu peninsula (Kaya, 1977; Yılmaz et al., 1994) without considering their possible tectonic significance. Şengör (1995) first suggested a possible Late Proterozoic oceanic connection between the Ural region in the east, through Northern Anatolia, to Eastern Europe in the west. Some studies recorded metamorphosed ultramafic and mafic magmatic rocks, and amphibolites of metasedimentary origin (e.g., Ustaömer, 1999).

The IZU is a discrete tectonostratigraphic terrane of the Turkish sector within the Alpine–Himalayan orogen. This terrane, or unit, has been variously termed the Istanbul–Zonguldak Unit (IZU) (Yiğitbaş et al., 1999); Istanbul–Zonguldak Zone (Yılmaz et al., 1997); the Istanbul Nappe (Şengör, 1984); or the Istanbul Zone (Okay, 1989). Metamorphic grades and deformation increase towards the lower part of the succession (Yiğitbaş and Elmas, 1997). The term "meta" for the basement associations is implicit in the following text, except where specific mineral assemblages are described.

Overlying the IZU metamorphic basement is a >3 km thick almost continuous sedimentary sequence ranging in age from lower Paleozoic, to Carboniferous. This sequence is at lower greenschist facies in the southern part of Almacık mountain, along the culmination of Sünnice Mountain and in the Armutlu peninsula (Fig. 1C; Abdüsselamoğlu, 1959; Yılmaz et al., 1994, 1997). The prevalence of metamorphic minerals and deformation increases towards the lower part of the Paleozoic succession (Yiğitbaş and Elmas, 1997).

The IZU Paleozoic sequence closely resembles Devonian–Carboniferous cover sequences observed at several localities in the southern part of the Hercynian chain: (1) in the Cantabrian Mountains of Spain, (2) Montagne Noire and Pyrenees, France, and (3) Sardinia. Similar possible ophiolite-cover sequences have also been described from the Carnic Alps, and the Krajstides of western Bulgaria (Görür et al., 1997). Ophiolitic fragments, overlain by early Paleozoic cover sequences are also known in the Variscan belt of Europe, as exemplified from the Tauern window (Eastern Alps), Carpathians, Balkans and Hellenides (Fig. 1A; Vavra and Frisch, 1989; Haydoutov, 1989; Kozhoukharova, 1996). They are regarded either as remnants of the Pan-African South European suture (Haydoutov, 1995), or alternatively as the Trans-European suture zone (Winchester, 2000).

The IZU differs in many features from the surrounding major tectonostratigraphic terranes; the Ballıdağ–Küre unit in the east, the Sakarya Continent in the south, and the Istranca massif to the west (Fig. 1B and C). The Ballıdağ–Küre Unit is a metamorphosed ophiolitic association of pre-Malm age, viewed as related to the Paleo-Tethyan Ocean (Şengör et al., 1984; Ustaömer and Robertson, 1994, 1997; Yiğitbaş et al., 1999). The IZU was thrust over the Ballıdağ–Küre Unit, prior to deposition of Upper Jurassic rocks as a common cover.

The Istranca massif, interpreted either as a part of the Cimmerian continent (Şengör, 1984; Yılmaz et al., 1997), or alternatively a Variscan fragment (Okay et al., 2001), is composed mainly of high-grade gneisses, schists, migmatites, and amphibolites, overlain unconformably by a metamorphosed Triassic cover sequence passing from conglomerate to phyllites, slates, and recrystallized limestones (Yılmaz et al., 1997). The western contact of the IZU with the Istranca massif in the west, concealed by Eocene sediments (Fig. 1B and C), has been interpreted as a transform fault (Okay et al., 1994), or a suture (Yılmaz et al., 1997).

The contact between IZU and the Sakarya zone is currently represented by the North Anatolian Transform Fault (NAF). The nature of this contact has variously been interpreted as: (1) a Neo-Tethyan suture zone (Intra-Pontide suture; Şengör and Yılmaz, 1981) prior to reactivation as North Anatolian Fault (NAF); (2) as a late Cretaceous high-angle fault zone (Yılmaz et al., 1994); or (3) as a late Cretaceous-Eocene strike-slip fault (Yiğitbaş et al., 1995, 1999; Elmas and Yiğitbaş, 2001).

Metamorphic basement associations in the IZU, of pre-Devonian, pre-early Ordovician or possibly Precambrian age have been recorded in the Çamdağ, Armutlu Peninsula, Almacık Mountain, Sünnice Mountain, and Karadere areas (Abdüsselamoğlu, 1959; Akartuna, 1968; Göncüoğlu et al., 1987; Yılmaz et al., 1981, 1990; Cerit, 1990; Yiğitbaş and Elmas, 1997; Ustaömer, 1999; Yiğitbaş et al., 1999). However, the primary geodynamic setting of these tectonostratigraphic fragments has remained unresolved (Table 1). In the following section metamorphic basement associations of the IZU, known collectively as the Sünnice Group (as a tectonostratigrahic unit), will be described from areas where they are best exposed.

2.1. Sünnice Group

Basement rocks of the IZU have been assigned different names in different areas (Table 1). In this

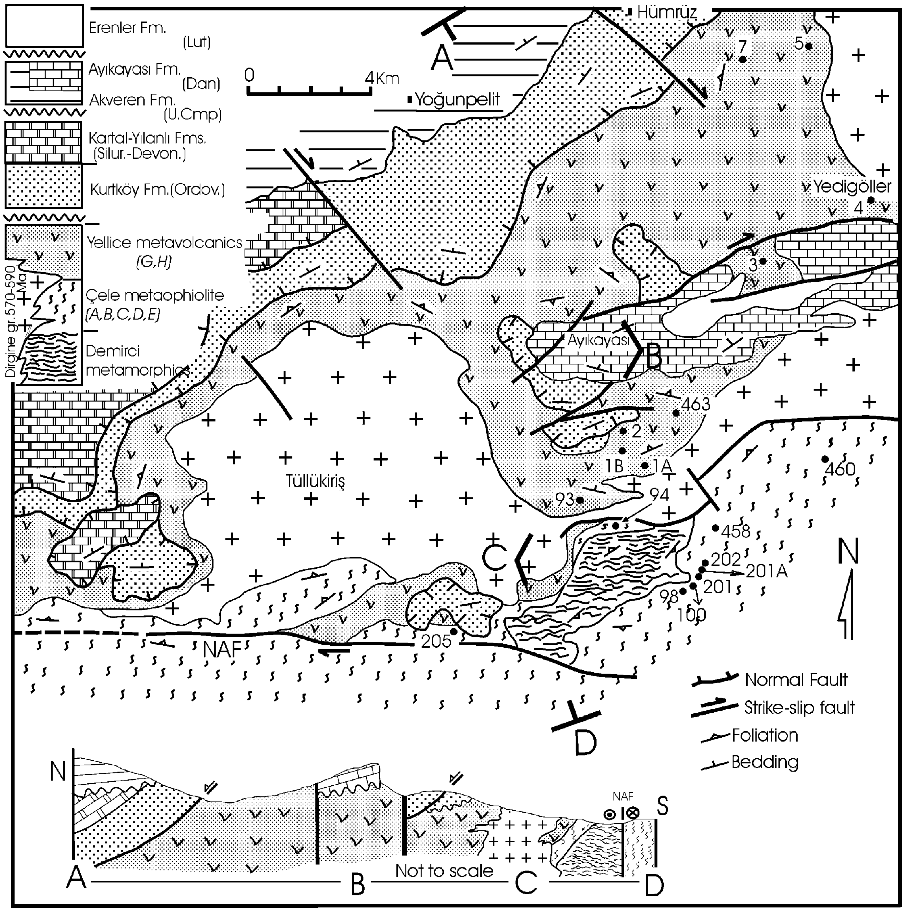

Fig. 2. Geological map of the Sünnice massif, and generalized N–S geological cross section. Italic letters in parentheses indicate the stratigraphic positions of the unit displayed in Fig. 5.

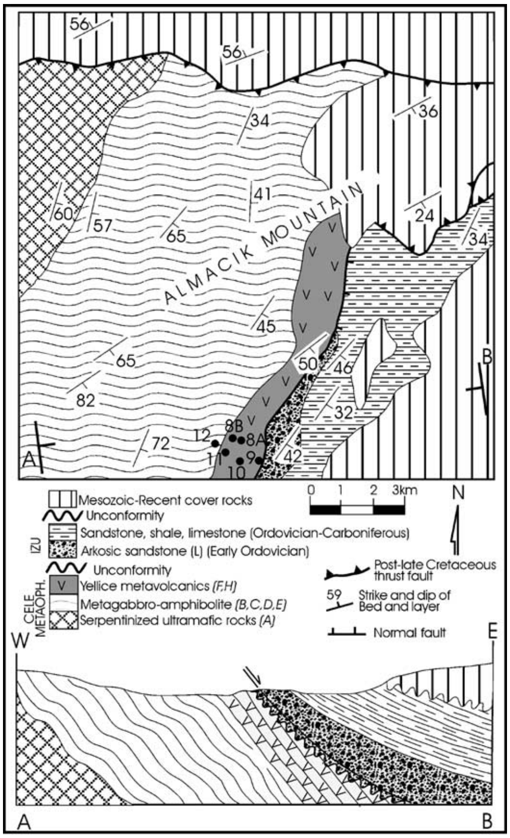

Fig. 3. Geological map of the Almacık Mountain and geological cross section (modified after Yılmaz et al., 1994). Italic letters in parentheses indicate the stratigraphic positions of the unit displayed in Fig. 5A–B: cross-section direction.

paper, this basement association is collectively termed the Sünnice tectonostratigraphic unit. It crops out along deeply eroded structural culminations beneath the thick Paleozoic cover sequence (Fig. 1C). Field, petrographical, and geochemical characteristics of the Sünnice terrane will be documented from the Sünnice, Almacık, and Armutlu areas (Figs. 2–4).

There are four major lithotectonic components of the composite Sünnice tectonostratigraphic terrane: the Demirci metamorphic sequence, Çele ophiolite, Yellice volcanic sequence, and Dirgine granite. The stratigraphic relations and the age constraints of the Sünnice Group is explained in Figs. 2–5 and the following related sections.

2.1.1. Demirci metamorphic sequence

The Demirci metamorphic sequence, exposed along the axis of NE–SW trending antiform in Sünnice Mountain, consists mainly of high-grade schists and migmatites (Fig. 2). The latter contains *ortho*-gneisses, with biotite, and biotite bearing amphibolites as thin interlayers. The gneisses display porphyroblastic texture, characterized by large megacrysts of plagioclase and K-feldspar within a more ductile fine- to medium-grained matrix of quartz, biotite and K-feldspar that is deflected around the megacrysts. These rocks are composed of the following mineral assemblages: plagioclase + biotite + quartz + amphibole + K-feldspar ± chlorite ± zircon (?). There are multiple generations of ductile to brittle deformation and metamorphism (Elmas and Yiğitbaş, 1998).

2.1.2. Çele ophiolite

The Çele ophiolite is exposed extensively in the Sünnice, Almacık, and Armutlu massifs. There is >2500 m thick sequence, from ultramafic rocks at the base to lavas interlayered with sedimentary rocks at the top, which we interpret as a near complete ophiolite pseudostratigraphy (Figs. 2–5). However, the proportions of the ophiolite lithologies vary between locations. Since most ophiolites contain a well-defined igneous stratigraphy as proposed in the Penrose ophiolite conference (Anonymous, 1972). Given the near complete pseudostratigraphy, and its presence in three areas (i.e. Sünnice, Almacık, Armutlu), we interpret it as the Çele ophiolite here. Fig. 5 is a tectono-stratigraphic column through the Çele ophiolite illustrating the composite generalised section derived from the field observation in all three areas.

Ultramafic rocks crop out more extensively in the Almacık Mountains, but are absent in the Armutlu peninsula (Figs. 2–5). In the Almacık Mountains, there is a thick ultramafic suite at the base of the Çele ophiolite, composed mainly of dunite, lherzolite, wehrlite and olivine websterite (Fig. 3). Chromite pods are locally present. Serpentinized ultramafic rocks have sporadic domains of magnesite, and some talc-magnesite, or magnesite-quartz mineral assemblages. Serpentinized ultramafic rocks grade into gabbroic amphibolites (Figs. 3 and 5). In the transition zone, leucocratic minerals are concentrated to form anorthosite and troctolite fractions. In contrast,

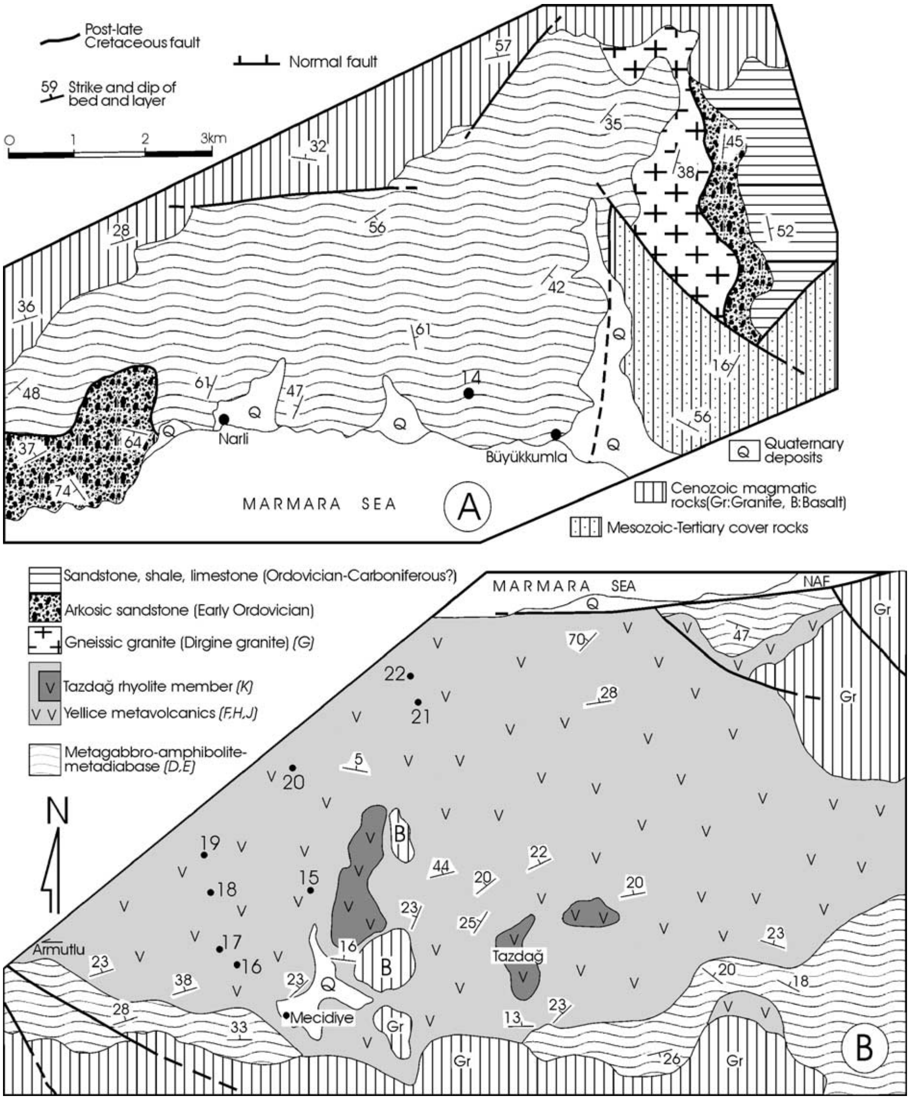

Fig. 4. Geological maps showing Precambrian rocks and cover units in the Armutlu massif. (A) Kumla area and (B) Tazdağ–Armutlu area. Italic letters in parenthesis indicate the stratigraphic positions of the unit displayed in Fig. 5.

ultramafic rocks in the Sünnice massif are represented by thin (<200 m) serpentinized peridotite slices, which were tectonically imbricated with deformed gabbro-amphibolite layers (Fig. 5). These ultramafic units are largely transformed into serpentinite. Rare relict orthopyroxene and olivine indicate that the protoliths were dunite, harzburgite, olivine-rich lherzolite, wehrlite, olivine websterite and clinopyroxenite. Cumulate banding and layering can be observed in several places despite the metamorphic overprint.

Coarse gabbroic amphibolite is prominent in the Çele ophiolite from all three areas. In the lower sections of the Sünnice area, around the contact with Demirci metaophiolite, the amphibolite is generally deformed in variable degrees to flaser, or a fine to medium banded, structure. The banding, formed from alternating layers of hornblende and plagioclase, resulted from ductile shear during metamorphism. In the mylonitized gabbro, deformed plagioclase and hornblende form augen structures within the mylonite ma-

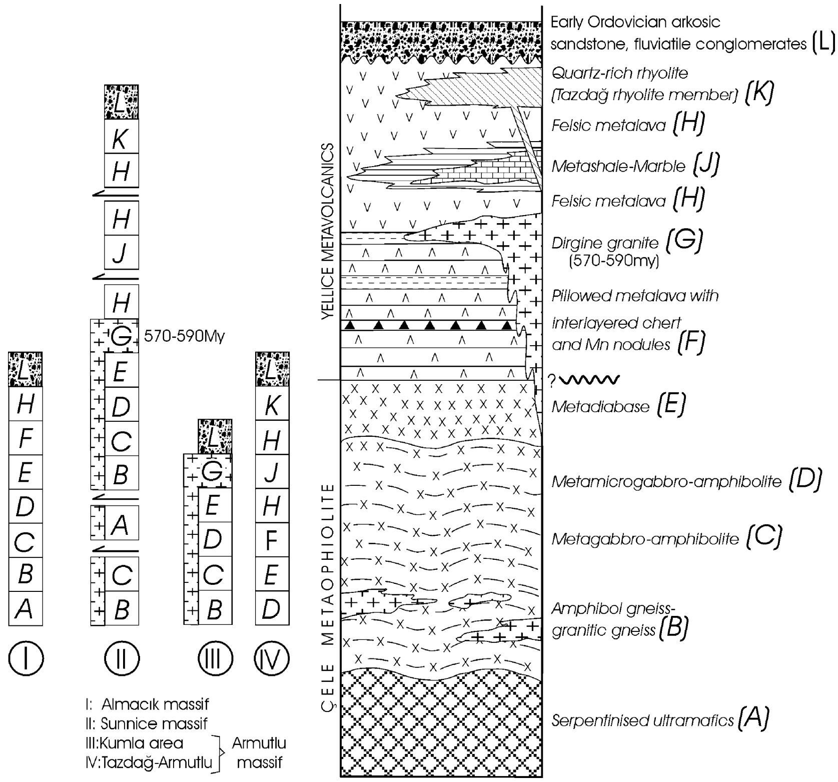

Fig. 5. Stratigraphic sections of the Çele ophiolite and the Yellice volcanics. Numbers indicate the mapping areas. Capital letters indicate the lithology which is seen in the field (schematic columns in the left) and their stratigraphic position in the palinspastically reconstructed composite stratigraphic column (to the right).

trix, which displays a well-developed interlocking mosaic texture. Chlorite and epidote minerals which are typical for greenschist metamorphism, overgrow and retrograde the older fabric. The rocks towards the structurally upper layers are characterised by massive, layered and highly strained gabbros, with plagiogranite sheets and veins. Massive gabbro comprises amphibolite facies minerals; hornblende porphyroblasts set within an plagioclase (An_{10-30}) matrix displaying gabbroic texture.

Layered metagabbros have a similar texture, but differ due to a coarse (up to 1 cm), parallel banding formed from variable modal proportions of hornblende porphyroblasts interpreted to represent primary igneous layering. Plagiogranite, in the form of streaks (in Sünnice and Armutlu areas), or anastomosing networks (Almacık area) occur within the upper part of the gabbroic amphibolite section. They occur as medium to coarse grained (0.1–1 cm) irregular bodies, up to 7 m thick, subparallel to the dominant tectonic foliation, having porphyroblastic red pyralspit garnet. The contact with the surrounding metagabbros are sharp, with no compositional or textural gradation.

Towards the upper part of the metagabbro sections, gabbro-amphibolites have relict ophitic textures, grading into fine-grained and dark-colored metadiabase (Fig. 5). These rocks may be distinguished from the overlying mafic rocks of the Yellice volcanic sequence in having coarse-grained, blasto-ophitic, or poikiloblastic texture. Least deformed amphibolites retain their original gabbroic structures and textures. In the eastern part of Sünnice Mountain, in the Kom valley, sheeted diabase dykes, about 50 cm wide, characterised by sharp boundaries, crop out. The dominant minerals are plagioclase, clinopyroxene, and rare orthopyroxene. Plagioclase is partially replaced by epidote and clinozoisite, whereas clinopyroxene is replaced by metamorphic green hornblend.

2.1.3. Yellice volcanics

In all three areas, at the top of the Çele metaophiolite is a greenschist metamorphic sequence, consisting of a range of volcanic rocks from basalt to rhyolites, and pyroclastic flows. Primary stratigraphic relations have been obscured during the metamorphism and younger phases of deformation in many areas; however, their original stratigraphy has been reconstructed as illustrated in Fig. 5, based on the field observations. Altered basalt lavas, with chert-radiolarite interbeds, occur at the base of the sequence, whereas dacite to rhyolites are abundant at the top. Basalt lavas show well-preserved pillow structures at the Bozburun area west of Armutlu (Eisenlohr, 1997). These rocks are represented by the greenschist facies mineral assemblage albite, epidote, chlorite and actinolite. Small volumes of chemical and siliciclastic sedimentary rocks, including marbles and shales, are generally present in the upper part of the section. Well-preserved quartz-rich felsic lava flows, in the uppermost part of the sequence, were mapped as the Tazdağ rhyolite member in the Armutlu peninsula (Figs. 4 and 5).

2.1.4. Dirgine granite

The Dirgine granite, which intrudes the metamorphic basement units, is composed mainly of granodiorite–tonalite. In the Sünnice (or Bolu) massif, Ustaömer (1999) described granitic rocks, termed the "Bolu Granitoid Complex", as pre-early Ordovician Cadomian arc-type granitoids. Hovewer, different granitic rocks in the area vary in age from Precambrian to Cretaceous. Accordingly, following Aydın et al. (1985) and Cerit (1990) we apply the name "Dirgine granite" for the Precambrian granodiorite–tonalite. Ustaömer and Rogers (1999) report ages ranging from 930 to 550 Ma for granitic rocks of the Sünnice area. Satır et al. (2000) and then, Chen et al. (2002) refined the ages of tonalitic and granodioritic rocks from the Karadere area to 570 and 590 Ma using U–Pb dating of zircon. Lastly, Ustaömer et al. (2003) calculated a new U–Pb of 571–579 Ma from the Sünnice massif which is critical since it sets an upper age limit to the rock groups intruded by these granites (Fig. 5).

3. Analytical methods

Major elements were determined by X-ray fluorescence spectrometry; data are reported on a volatile free basis. Inductively coupled plasma atomic emission spectrometry (ICP-AES) was used to determine Cr, Co and Ni; detection limits are 1 ppm. Rare earth elements (REE), high-field strength elements (HFSE) and other trace elements listed were analyzed by inductively coupled plasma mass spectrometry (ICP-MS, Perkin-Elmer Elan 5000) in the Department of Geological Sciences, University of Saskatchewan, using the method of Jenner et al. (1990), with standard additions, pure elemental standards for external calibration, and BIR-1, BHVO-1, and SY-2 as reference materials. Wet chemistry operations were conducted under clean laboratory conditions. Samples were analyzed twice using both HF–HNO_3 acid dissolution and Na_2O_2 sinter techniques (Jenner et al., 1990; Longerich et al., 1990) to avoid possible problems associated with HFSE and REE in refractory minerals. The detection limits, defined as 3σ of the procedural blank, for some critical elements, in parts per million, are as follows: Th (0.01), Nb (0.006), Hf (0.008), Zr (0.004), La (0.01), Ce (0.009), Nd (0.04), and Sm (0.03). Precision for most elements at the concentrations present in BIR-1 is between 2 and 4% R.S.D., excepting Nb (R.S.D. 6%). Chondrite and primitive mantle normalizing values are taken from McDonough and Sun (1995, and references therein). Nb/Nb*, Zr/Zr*, Hf/Hf*, and Ti/Ti* are calculated relative to neighboring REE, as for Eu/Eu*.

4. Results

Based on major element compositions and petrographic observations, magmatic rocks of the Sünnice Group have been divided into four groups: (1) ultramafic rocks, (2) gabbro-amphibolites, (3) mafic volcanic rocks, and (4) intermediate to felsic volcanic rocks. The first two groups belong to the "Çele ophiolite", their first detailed geochemical properties are given here, whereas the second two are from the "Yellice volcanic sequence" (Tables 2 and 3). In the Nb/Y versus SiO_2 diagram (Winchester and Floyd, 1977) these rocks show a complete subalkaline spectrum from basalt to rhyolite (Fig. 6). Using the classification of Gill (1981) and Bailey (1981), the volcanic suite from basalt to rhyolite display similar characteristics to recent orogenic counterparts, with $Zr = 35–250$, $Ce < 75$ ppm, $Nb/Y = 0.8$, $K_2O <$

Table 2
Summary of the analyses of 30 samples

	Çele ophiolite		Yellice volcanic association		
	Ultramafic rocks	Gabbroic amphibolites	Mafic volcanic rocks		Intermediate and felsic volcanic rocks
			Sünnice type	Armutlu type	
SiO_2	41.7–50.6	46.3–51.4	53.2–55.9	49.1–51.0	58.4–78.1
TiO_2	0.034–0.155	0.456–2.971	1.108–1.517	1.468–1.769	0.175–0.946
Fe_2O_3	8.0–15.4	10.4–15.7	11.7–14.3	10.1–11.7	2.78–15.54
MgO	23.1–39.8	6.6–11.0	4.1–5.4	7.0–7.8	0.6–4.2
K_2O	0.037–0.104	0.184–1.248	0.145–0.485	0.084–0.388	0.092–3.119
Mg#	85–86	48–69	0.42–0.48	0.57–0.63	0.23–0.49
Cr	2242–2996		8.0–11.0	127–261	
Co	54.0–158.0		0.9–28.7	9.3–56.2	
Ni	689–2077		1.0–19.0	55–87	
Ba	5.84–7.70	45.72–869.7	20.95–229.96	8.70–33.14	28.86–900.35
Zr	1.13–4.68	8.47–62.49	67.51–116.30	47.32–96.85	19.07–207.23
Ce	0.165–1.307	2.382–41.327	16.84–44.56	13.805–15.232	8.973–42.818
$(La/Yb)_{cn}$	1.67–4.22	0.95–2.76	1.38–4.10	1.19–1.36	1.06–4.99
$(La/Sm)_{cn}$	1.19–3.36	0.85–1.66	1.10–1.43	0.80–0.91	1.04–2.81
$(Gd/Yb)_{cn}$	0.91–1.22	0.95–1.79	1.16–2.53	1.33–1.45	0.79–1.47
Al_2O_3/TiO_2	53.70–57.99	4.54–38.28	11.70–13.90	8.31–10.47	12.91–65.91
Th/Nb	0.34–0.91	0.24–1.25	0.46–0.71	0.06–0.31	0.58–2.45
Th/La	0.08–0.39	0.05–0.15	0.09–0.23	0.05–0.11	0.30–0.43
Zr/Y	1.84–8.87	0.54–1.53	1.68–2.6	1.56–3.40	1.36–8.25
Ti/Zr	171–218	209–449	74.85–101.26	89.13–196.60	5.05–210.86
Ba/Zr	1.25–5.59	2.19–51.99	0.31–3.74	0.11–0.35	0.44–13.82
Ti/V	7.07–9.09	9.63–49.73	22.08–66.90	27.06–29.95	11.62–191.35
Sc/Y	5.37–59.65	0.85–7.28	0.71–1.22	1.41–1.77	0.36–2.85
Ce/Yb	5.33–10.79	3.62–9.58	4.88–11.6	4.83–5.41	3.49–14.16
Zr/Rb	9.04–25.25	0.32–17.13	15.83–65.63	10.44–103.83	0.84–85.60
Nb/Nb*	0.08–0.45	0.11–0.43	0.13–0.35	0.24–0.98	0.07–0.86
Eu/Eu*	3.93–4.59	0.81–1.44	0.65–0.97	0.94–1.02	0.40–0.99
Zr/Zr*	0.60–2.43	0.18–0.46	0.33–0.68	0.48–1.11	0.46–2.21
Hf/Hf*	0.76–3.99	0.15–0.49	0.37–0.79	0.39–1.31	0.48–2.99
Ti/Ti*	1.09–4.68	0.51–1.41	0.33–0.59	0.85–0.88	0.11–0.92

Values show maximum and minimum for each group.

5 wt.%, and $TiO_2 < 1.75$. Mafic volcanic rocks and amphibolites are all tholeiitic.

4.1. Alteration insensitive elements

It is known that the majority of Precambrian magmatic rocks have undergone metamorphism and/or metasomatism, resulting in chemical alteration. Al_2O_3 TiO_2, P_2O_5, HFSE (Th, Nb, Ta, Zr, Hf, Y), and REE are generally considered to be relatively immobile up to amphibolite facies, whereas, MgO, CaO, Na_2O, K_2O, and LILE (Cs, Rb, Ba), are considered to be relatively mobile, albeit LREE may be more alteration sensitive than HFSE and HREE (Floyd and Winchester, 1975; Humphris and Thompson, 1978; Dostal et al., 1980; Hynes, 1980; Ludden et al., 1984; Campbell et al., 1984; Murphy and Hynes, 1986; MacLean and Kranidiotis, 1987; Middelburg et al., 1988; Smith, 1992; Polat and Hofman, 2003; Polat et al., 2003). Thus, in this paper, magmatic rocks of the Sünnice Group are characterized on the basis of the alteration insensitive elements and these elements are then used to constrain their geodynamic setting (Figs. 6–10). Although, LREE may be slightly more

Table 3
Summary of the characteristics of mostly Precambrian ophiolites in eastern Europe, along the South European suture zone

Region	Reference	Lithology	Ages	Interpretation
Eastern Alps	Neubauer et al. (1989), Vavra and Frisch (1989)	Stubach complex: ultramafic rocks, gabbroic and basaltic amphibolites	Late Precambrian to early Paleozoic	A back-arc oceanic crust
		Ritting complex: amphibolites accompanied by sheared serpentinite lenses	Pre-late Ordovician	A disrupted MORB-type ophiolite
		Speik complex: metamorphosed peridotite, ultramafic and mafic cumulates, sheeted dikes, extrusives and oceanic sediments from base to top	Covered by a Silurian metapelites depositionally	A back-arc oceanic litosphere
		Plankogel complex: serpentinite, amphibolites, micaschist, alkali basalt, manganiferous chert	Late Precambrian (prior to 700 Ma)	A tectonic mélange
		Storz Group: banded gneiss intercalated with basaltic amphibolites and its acid differentiates; gabbroic amphibolites with ultramafic slices	Pre-Variscan/Rheic (?)	A primitive island arc
		Habach Group: amphibolites derived from low-K basaltic andesites; dacite, rhyolite, pelagic metasediments, volcaniclastics		An ensimatic island arc
Bohemian massif	Jelinek et al. (1984)	Letovice Ophiolite: ultramafic, mafic, and sedimentary rocks in greenschist to amphibolite facies	Late Proterozoic	MORB or back-arc setting ophiolites
	Kastl and Tonika (1984); Bowes and Aftalion (1991)	Marianske Lazne complex: eclogites, serpentinites, metagabbros, amphibolites	Latest Proterozoic–early Paleozoic (Bowes and Aftalion, 1991)	
Rhodope massif	Kozhoukharova (1996)	Rhodope ophiolitic association: eclogites, serpentinites, gabbros, amphibolites, micaschists, marbles	Middle Riphean	Oceanic crustal fragments obducted over the active edge of an ancient continent
South Carpathian–Balkan	Haydoutov (1989, 1995)	Berkovica Group: tectonized peridotite, layered cumulates, sheeted dikes, pillow lavas, tholeiitic-calc-alkaline lavas and a volcani–clastic sedimentary sequence	Proterozoic ophiolite; Cambrian volcaniclastic sediments	A complete ophiolitic succession (MORB) and an ensimatic island arc association
Western Pontides	This paper	Çele metaophiolite and Yellice volcanics	Precambrian	Suprasubduction zone ophiolite, ensimatic island arc, and back-arc basin associations

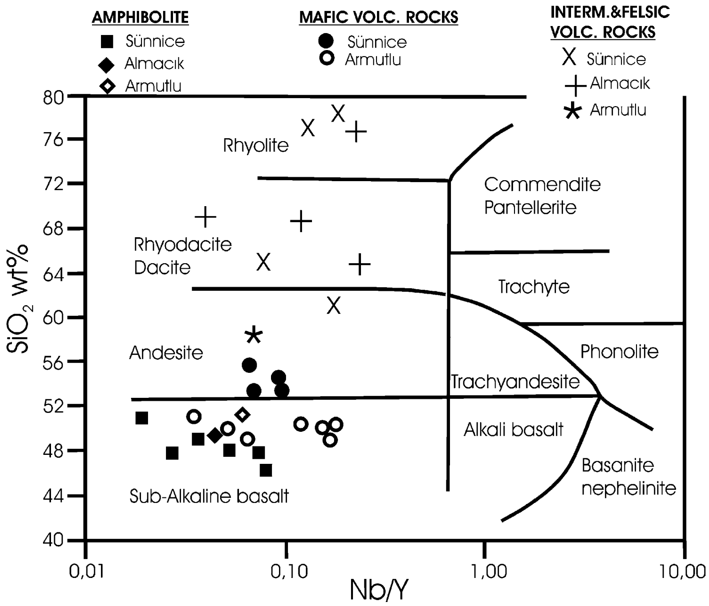

Fig. 6. Binary plots of SiO_2 vs. Nb/Y diagram for Çele ophiolite amphibolite and Yellice volcanics.

mobile than HFSE, yet, for example, Th/Ce ratios are generally uniform in Sünnice amphibolites and mafic volcanic rocks ruling out significant LREE mobility (Data repository in Appendix A).

4.2. Ultramafic rocks

Due to pervasive serpentinization, only a few selected analyses were conducted on the ultramafic rocks of the Çele ophiolite. They have high MgO at 23–39 wt.%, Mg#; 85–86, Cr 2242–2996 ppm and Ni; 689–2077 ppm contents (Table 2). Intense alteration is reflected in positive Eu anomalies, and an Hf/MREE fractionation in sample EY201 (Fig. 7). REE plot at ~1 times chondrite.

4.3. Amphibolites

Petrographically, amphibolites of the Çele ophiolite are dominated by modal plagioclase and amphibole. This group is characterized by a narrow range of SiO_2 from 46 to 51 wt%, and Mg# spans 69–48. Al_2O_3/Ti_2O ratios vary between 4.5 and 20 (except two outliers EY94 = 38.28 and EY14 = 26.89; Table 2 and Data repository in Appendix A). Their Ti/Zr ratios (209–449) are greater than chondritic. In the Nb/Y versus SiO_2 diagram, all of the amphibolites plot in the sub-alkaline basalt field (Fig. 6).

Representative chondrite-normalized REE are plotted on Fig. 7c. Rare earth elements plot at about 10 times chondrite, with two flat patterns, and two with fractionated HREE. Minor negative to positive Eu anomalies are present ($Eu/Eu^* = 0.81$–1.44). On primitive mantle-normalized diagrams, there are systematic negative anomalies at Nb–Ta and Hf–Zr. This characteristic has been explained in terms of retention of these immobile elements (conservative elements—Pearce and Peate, 1995) reflecting the extent of depletion of the mantle wedge source during partial melting (Wilson, 1993), whereas the non-conservative elements such as LREE and LILE's from the subduction component were enriched (Pearce et al., 1999). LREE depletion in sample EY100 may be due to alteration, or more likely may reflect an extremely depleted mantle source, given that both Th and Ce have normalized abundances less than Nd (Fig. 7c and d).

4.4. Mafic volcanic rocks

In the Armutlu area, mafic volcanic flows are compositionally uniform tholeiitic basalts. SiO_2 spans

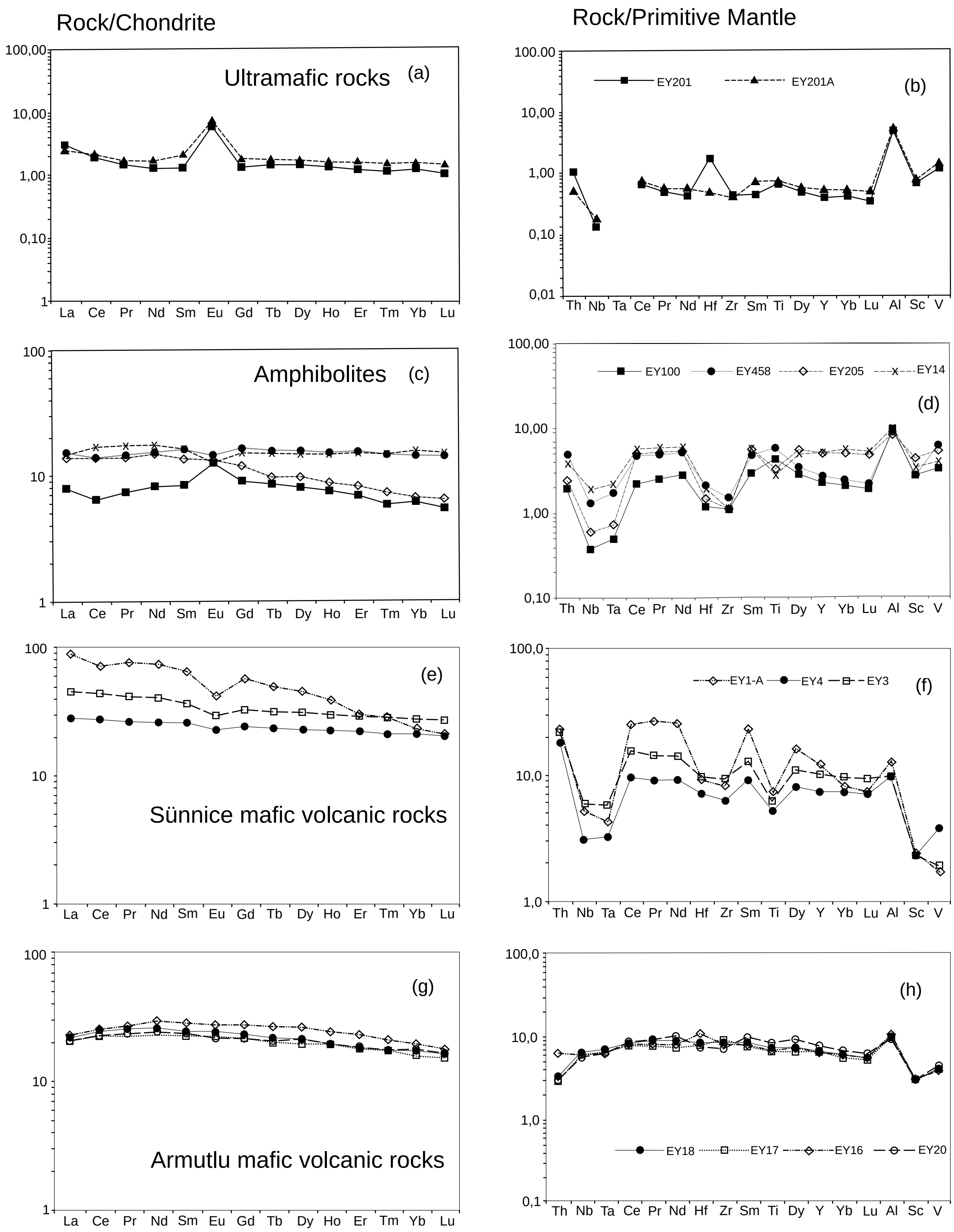

Fig. 7. Chondrite-normalized REE's and multi-element primitive mantle normalized spiderdiagrams for ultramafic rocks and amphibolites of Çele metaophiolite, and Armutlu mafic volcanic rocks of Yellice volcanics.

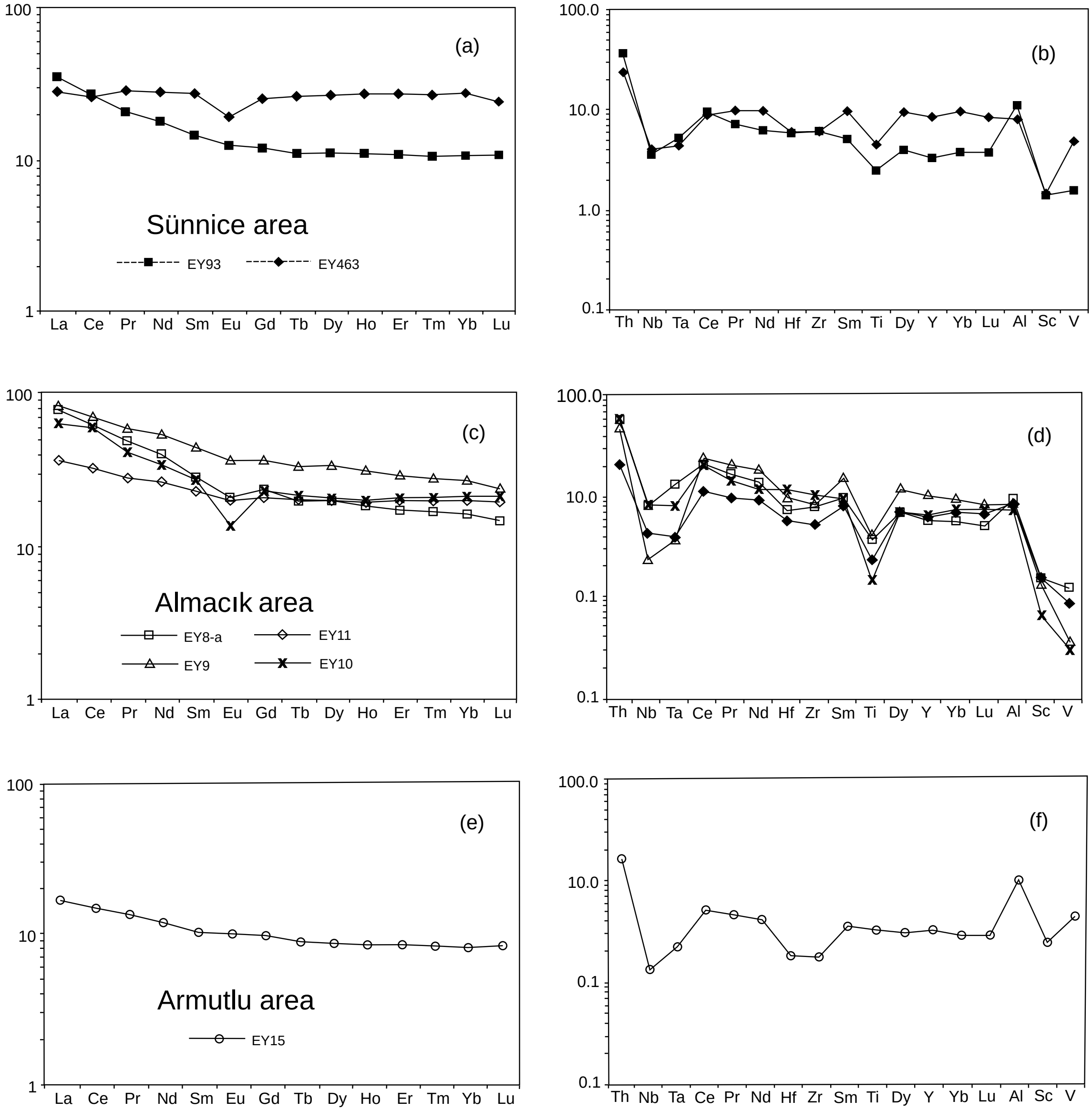

Fig. 8. Chondrite-normalized REE's and multi-element primitive mantle normalized diagrams for intermediate and felsic volcanic rocks of Yellice volcanics.

49–51 wt.%, Mg# ranges from 63 to 57, and Ni contents are 87 to 55 ppm (Table 2 and Data repository in Appendix A). Rare earth elements are about 20 times chondrite (Fig. 7g). REE and primitive mantle normalized diagrams feature: (1) LREE depletion; (2) fractionation of HREE, where $(La/Yb)_{cn} = 1.2$ to 1.4; and (3) codepletion of Th with Nb and LREE (Fig. 7h). They plot in the intraoceanic arc field of Hawkesworth et al. (1993), but lack the negative anomalies at Nb–Ta, or Ti of primitive arc tholeiites. The basalts are compositionally similar to normal mid ocean ridge basalts (NMORB), albeit with less incompatible element depletion.

Mafic flows in the Sünnice area are compositionally more variable, collectively tholeiitic and subalkaline to calc-alkaline: SiO_2 and Mg# range from 53 to 56 wt.%,

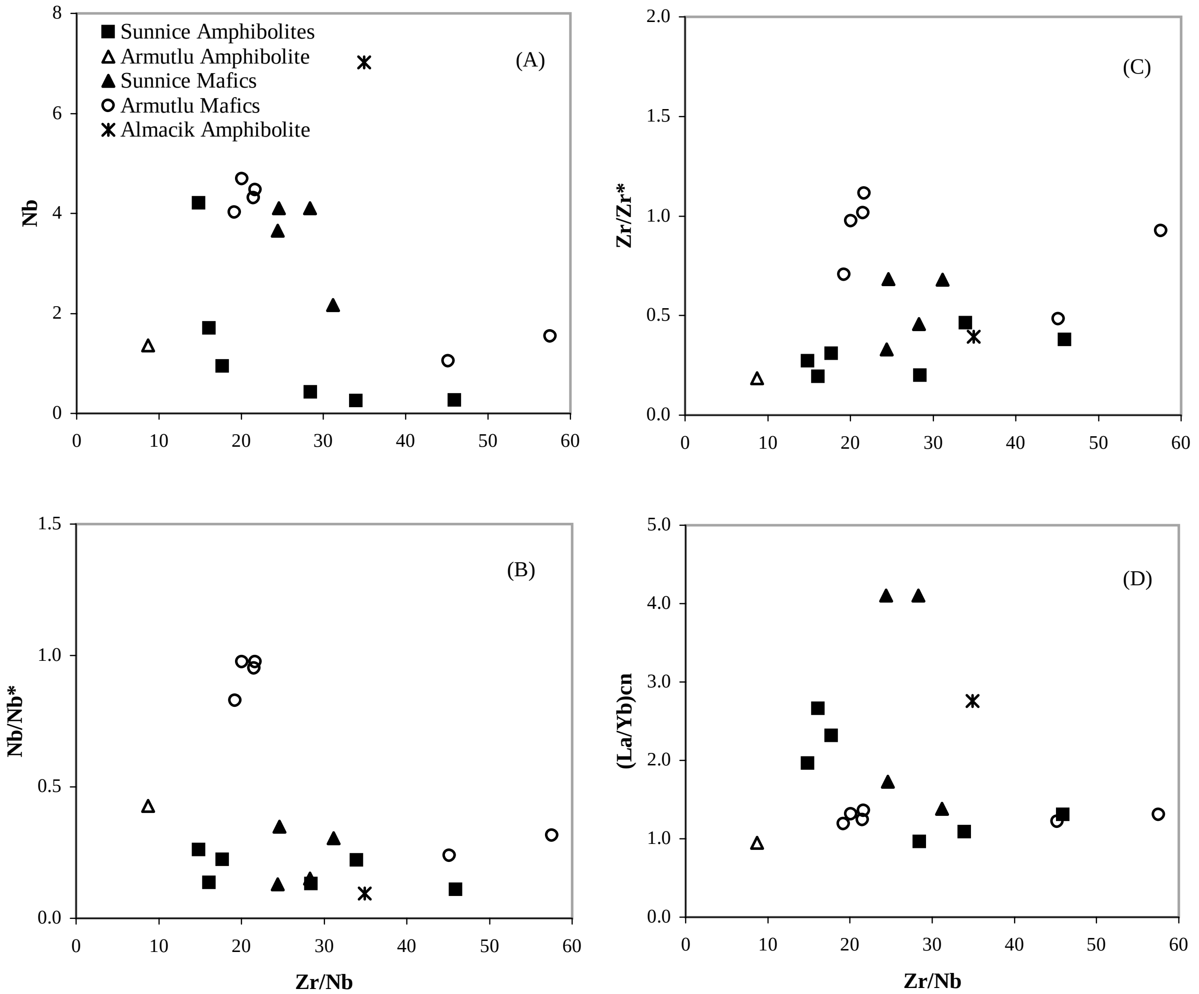

Fig. 9. Plots of Zr/Nb vs. Nb (A), Nb/Nb* (B), Zr/Zr* (C), and $(La/Yb)_{cn}$ (D).

and 48 to 42, respectively. Chromium, Co, and Ni contents are consistently lower than in Armutlu counterparts, consistent with a calk-alkaline fractionation trend (Table 2 and Data repository in Appendix A). There is a spectrum of REE contents and fractionations from $(La/Yb)_{cn} = 1.4$ to 4.1; with increasing REE fractionation there are progressively larger negative anomalies of Nb–Ta, Hf–Zr, and Ti relative to neighboring REE indicative of a convergent margin setting.

4.5. Intermediate and felsic volcanics

Intermediate and felsic flows are associated with mafic counterparts in the uppermost sections of the Yellice volcanic sequence in all three areas. Compositions range from $SiO_2 = 58$ to 78 wt.%, Mg# 23 to 49, $TiO_2 = 0.175$ to 0.946, Zr = 19 to 207 ppm, and $Al_2O_3/TiO_2 = 13$ to 65 (Table 2). Collectively, these rocks plot in the andesite, rhyodacite, and rhyolite fields on the Nb/Y versus SiO_2 diagram (Fig. 6).

Two dacites from the Sünnice area differ in trace element characteristics. One has a flat REE pattern at ~30 times chondrite, whereas the second has fractionated LREE (Fig. 8a and b). The former is likely a tholeiitic dacite, from extensive fractional crystallization of a parental tholeiitic basalt liquid, whereas the latter is a fractionated calc-alkaline basalt, in the arc basalt–andesite–dacite–rhyolite (BADR) fractionation trend.

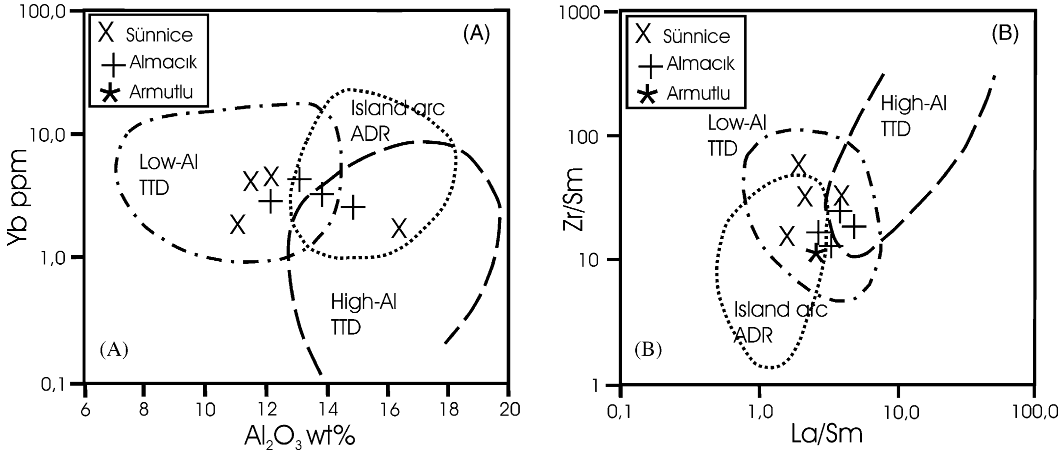

Fig. 10. Data for intermediate and felsic volcanic rocks data plotted in Al_2O_3 vs. Yb (A), and Zr/Sm vs. La/Sm (B) coordinates. Low-Al trondjhemite–tonalite–dacite (TTD), high-Al TTD, Island-arc andesite–dacite–rhyolite (ADR) (modified after Drummond et al., 1996).

Dacites to rhyolites in the Almacık area form a compositionally coherent group, with La at 35–80 times chondrite (Fig. 10A and B). Two samples have flat HREE, whereas two show fractionated HREE, a variation also seen in both the amphibolites and Sünnice mafic volcanic rocks (Fig. 7c–f). The former are likely fractionation products of basaltic liquids generated in the mantle wedge above 80 km, and the latter from basaltic liquids formed below 80 km, with residual garnet. All samples have pronounced negative anomalies at Nb–Ta, and Ti. These troughs are some combination of anomalies inherited from arc basalts with HFSE/REE anomalies, and fractional crystallization of a titanite phase. There are flat pattern to negative anomalies at Hf–Zr. Negative anomalies are either inherited from parental basalts, as seen in some Sünnice mafic flows, and/or stem from fractionation of zircon. A single andesite from the Armutlu area is compositionally similar to Almacık counterparts with fractionated HREE. A consistent feature of this intermediate to felsic volcanic suite are large normalized enrichments of Th relative to Ce (Fig. 8).

5. Discussion of the geochemical features of the Çele ophiolite and Yellice volcanics

5.1. Influence of alteration and crustal assimilation

Each group of rocks shows generally coherent REE and primitive mantle normalized patterns indicative of the retention of primary compositional features for these alteration insensitive elements. Minor positive to negative Eu anomalies in some of the amphibolites and Sünnice mafic volcanic rocks likely reflects seafloor hydrothermal alteration. The most conspicuous alteration feature is pronounced fractionation of Nb–Ta or Hf–Zr, or both in some samples. Tantalum is enriched in the amphibolites EY460 and EY98; Zr enriched relative to Hf in Sünnice basalt EY1-B; and Nb and Hf depleted relative to Ta and Zr, respectively in Armutlu basalt EY21. In these samples, alteration does not appear to have influenced REE patterns, Eu excepted, or Th; for example, Th/Ce ratios are uniform in six amphibolites that include three with Nb/Ta fractionations, and are uniform in six Armutlu mafic volcanic rocks including having two Zr/MREE and Zr/Hf fractionations (Data repository in Appendix A). The following discussion is restricted to samples without Nb–Ta or Hf–Zr fractionations.

It is difficult to gauge the presence of crustal contamination in arc amphibolites and basalts, given that intraoceanic arc magmas and continental crust are both characterized by the conjunction of LREE fractionation, with LILE/LREE, and HFSE/REE fractionations (Taylor and Mc Lennan, 1985; Pearce and Peate, 1995, and references therein). We note that the amphibolites and basalts plot with intraoceanic arcs, rather than continental margin arcs, in Ce–Yb co-ordinates of Hawkesworth et al. (1993). In addition, the magnitude of the negative Nb anomaly in amphibolites

(Fig. 7d) and Sünnice mafic volcanics does not deepen with increasing SiO_2 or Ce, nor does La/Yb_{cn} covary with SiO_2, as would be expected for progressive contamination by continental crust. In addition, Armutlu mafic volcanic rocks are devoid of negative Nb–Ta or Ti anomalies (Fig. 7h). Accordingly, we interpret Sünnice, Almacık, and Armutlu mafic rocks to have formed in an intraoceanic setting.

5.2. Characteristics of the mantle wedge

The composition of subduction-related basalts is considered to be controlled by two sources; the wedge, and subduction components (Pearce and Peate, 1995, and references therein). The HFSE, which are insoluble in subduction derived fluids, are inherited from the mantle wedge (McCulloch and Gamble, 1991; Woodhead et al., 1993; Pearce and Parkinson, 1993). Fluids driven off the slab into the mantle wedge are enriched in LILE over LREE, and in LREE over the conservative HFSE, giving the characteristic compositional features of arc basalts (Perfit et al., 1980; Tatsumi et al., 1986; Morris et al., 1990; Hawkesworth et al., 1993).

Accordingly, the negative Nb and Hf anomalies of the Sünnice ultramafic and mafic rocks, and Almacık amphibolite, can be interpreted in terms of a suprasubduction zone setting (SSZ). These LREE/HFSE fractionations indicative of a SSZ, have also been documented in 2.7 Ga volcanic sequences of Superior provence, Canada (Polat et al., 1999; Polat and Kerrich, 2002).

Most Phanerozoic and Recent arc, and back-arc basalts have Nb contents of 1 to 2 ppm (Taylor, 1992; Ewart et al., 1994; Pearce and Peate, 1995; Elliot et al., 1997). According to Pearce and Peate (1995), HFSE ratios of arc basalts are generally within the MORB array. However, the total range of Zr/Nb in primitive arcs is 9–87, versus 32 for average MORB (range 11–87), signifying mantle sources variably depleted or enriched relative to average MORB (Davidson, 1996; Macdonald et al., 2000).

Tholeiitic basalts, and amphibolites of the Sünnice Group are distinct in having variable Nb contents, and Zr/Nb, ratios that reflect the previous extent of depletion or enrichment of the mantle wedge. Armutlu basalts are characterized by Nb contents of 1.05–4.5 ppm, where Zr/Nb ratios decrease from 57 to 20 with increasing Nb. Sünnice counterparts have Nb 2.2–5.1 ppm, and Zr/Nb 24–31. Collectively, amphibolites possess Nb contents spanning 0.26–4.2 ppm, where Zr/Nb ratios of 9–46 also decrease with Nb abundance (Table 2 and Data repository in Appendix A).

Generally, the lowest values of Nb, and Nb/Nb* correspond to the largest Zr/Nb ratios, and negative Zr(Hf)/MREE anomalies. Accordingly, the mantle wedge from which the Sünnice Group formed was heterogeneous relative to average Phanerozoic MORB. Varying from extremely depleted by previous melt extraction events leaving a refractory residue (high Zr/Nb), and subsequently locally enriched by a subduction related component (deep Nb anomaly), to a less refractory mantle wedge (low Zr/Nb) in conjunction with a lower degree of subduction enrichment (Fig. 9; cf. Pearce et al., 1999). However, amphibolites and basalts with higher Nb contents do not qualify as Nb-enriched basalts (NEB), where Nb abundances are >10 ppm (Sajona et al., 1996).

5.3. Sediments on the slab?

In a convergent margin setting, where sediments on the slab melt magmas acquire high Th/Ce but high Ta/Nb ratios relative to fluid dominated melts (Hawkesworth et al., 1977; Elliot et al., 1997; Macdonald et al., 2000). Mafic rocks from Sünnice and Armutlu basalts plot on the low Ce trend of intraoceanic arc basalts of Hawkesworth et al. (1993). Sünnice mafic rocks have Th/Ce ratios that range from 0.02 to 0.09, whereas the upper limit for intraoceanic arcs with minimal sediment input is 0.01–0.02. The Th/Ce ratios do not correlate with Ce content. Consequently, it is that sediments on the oceanic slab of the Sünnice arc melted. In contrast, Th/Ce ratios are systematically lower in Armutlu basalts, averaging 0.02. Along the Mariana arc, sectors dominated by slab dehydration-wedge melting have Ta/Nb ratios less than 0.06, whereas sectors with sediment melting feature larger ratios (Elliot et al., 1997). Both the Sünnice and Armutlu mafic rocks have Ta/Nb ratios of 0.06 or less consistent with fluid dominated melting. Consequently, there is conflicting evidence for sediment input to the Sünnice arc, but the Armutlu arc was fluid dominated.

5.4. Co-magmatic relationships

Andesites, dacites, and rhyolites in all three areas show compositional trends consistent with co-magmatic relationship with Sünnice mafic volcanics. They share the HFSE/REE fractionations with the mafic rocks that collectively are indicative of convergent margin magmatism. The Th and LREE contents, and Th/LREE ratios are comparable to evolved magmas from intraoceanic settings, rather than continental margins, in keeping with the interpretation drawn for mafic parental liquids (cf. Hawkesworth et al., 1993).

Intermediate to felsic rocks span the low Al TTD and Island arc ADR series, overlapping marginally with the high Al TTD series of Drummond et al. (1996) (Fig. 10). The latter are prevalent in the Archean and Paleoproterozoic, where high Al granitoids form by slab melting with residual garnet, to give low Yb and strongly fractionated HREE. Collectively, the intermediate and felsic rocks have mildly fractionated HREE, relatively low Al, but greater Yb than high Al TTD. They evolved by fractional crystallization from the arc basalts that were products of slab dehydration-wedge melting, under lower thermal gradients than slab melting.

All of the Sünnice mafic rocks and the Armutlu basalts are characterized by fractionated HREE, indicative of residual garnet. Fractionated HREE is not observed in most Phanerozoic arc basalts, but has been recorded in Precambrian arcs (Pearce and Peate, 1995; Hollings and Kerrich, 2000; Polat and Kerrich, 2001a), signifying depths of greater than 80 km. Pronounced negative Hf–Zr fractionation relative to MREE is also not seen in most arc tholeiitic basalts. It is thought to result from extreme hydrous metasomatism of the mantle wedge, under conditions where Zr and Hf are more conservative than MREE.

6. Geological evolution of the Sünnice Group

6.1. Age of the Sünnice Group

In most the outcrops in the Sünnice, Almacık, and Armutlu massifs the contacts of the Sünnice Group with the overlying early Ordovician Kurtköy formation continental clastics is low angle normal faults that developed along the unconformity surface (Figs. 2–5). However, in the Çamdağ and Karadere areas (Fig. 1C) the contact is normal across a surface of an unconformity (Arpat et al., 1978; Aydın et al., 1985; Boztuğ, 1992).

The lowermost continental deposits of the Paleozoic sequence were previously identified as Cambrian by Arpat et al. (1978) and Aydın et al. (1985). The age of the Sünnice Group was attributed to the Precambrian (Arpat et al., 1978; Aydın et al., 1985; Kaya, 1977; Yılmaz et al., 1997). However, the age of these red clastics was shown more recently to be pre-Arenig-Llanvirn (Dean et al., 1997), and hence the Sünnice Group must be pre-Ordovician. However, since the Dirgine granite cuts and post dates the tectonic amalgamation of the Sünnice Group in the Sünnice area, the latter is clearly Neoproterozoic and older than 570–590 My (Chen et al., 2002; Ustaömer et al., 2003).

6.2. Exhumation history of Sünnice Group

The metamorphic grade of the Sünnice metamorphic rocks decreases steadily upwards from amphibolite facies to greenschist facies. This is mainly due to the last major phase of metamorphism during early Cretaceous (Yiğitbaş et al., 1999). In the Sünnice, Almacık, and Armutlu massifs, the overlying Paleozoic sequence also shows low-grade metamorphism to the lower limit of the greenschist facies. The rocks were foliated, and partly recrystallized. Metamorphism and low intensity deformation did not destroy primary sedimentary features of the Paleozoic clastic sequence. Clasts vary in size from mm to 5 cm, and were derived from granites, quartz-rich felsic volcanic rocks, spilitized volcanic rocks, and green-grey shales, rock-types seen in the underlying Yellice volcanics and the Dirgine granite. No clastic derivatives from the Çele ophiolite have yet been observed (Yılmaz et al., 1981; Yiğitbaş and Elmas, 1997).

The clasts of Ordovician rocks along the contact commonly display cataclastic deformation. Wherever the tectonic contact is seen between the Sünnice Group and the Paleozoic cover rocks, it is a major, north dipping normal fault along which a wide extensional shear zone was developed. Closer to the contact, the mylonitized wall-rocks display increasing dynamic metamorphism; the conglomerates of the Kurtköy forma-

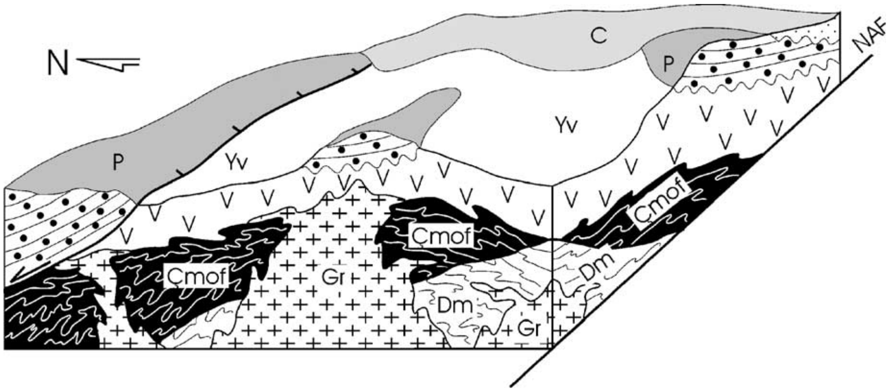

Fig. 11. Block diagram showing the relation between Sünnice Group and cover rocks. Abbreviations: C, early Cretaceous sedimentary successions; P, Paleozoic sequence; Gr, Dirgine granite; Yv, Yellice volcanics; Çmof, Çele ophiolite; Dm, Demirci metamorphics.

tion developed cataclastically deformed gneissose textures. This structural relationships indicate that the Paleozoic sequence, which was initially deposited above the Sünnice Group rocks, was later detached along a low-angle listric normal fault (Fig. 11).

The first common cover sedimentary succession, the Ulus Group, which covers both the Sünnice Group and the Paleozoic sequence is the Lower Cretaceous (Yiğitbaş et al., 1999), was interpreted to have been deposited within a newly developed extensional basin. Extension affected the regionally deformed, uplifted and eroded terrane. According to previous studies (Görür et al., 1993; Görür, 1997) the Ulus basin may be linked to the initial stage of rifting of the Western Black sea basin, which occurred during the late Berriasian–Valanginian period (Yiğitbaş and Elmas, 1997; Georgescu, 1997; Yiğitbaş et al., 1999).

7. Geodynamic implications and conclusions

Diverse metamorphic rocks of the Sünnice Group crop out in many inliers in Northwestern Anatolia, Turkey, in the basement of IZU (Fig. 1). These metamorphic rocks display features that may link them either to the pre-Variscan metamorphic basement association of Europe (Frisch and Neubauer, 1989; Haydoutov, 1989; Neubauer et al., 1989; Vavra and Frisch, 1989; Kozhoukharova, 1996), or to the early to middle Proterozoic oceanic environment in the Mediterranean and Middle East regions (Lev and Arkady, 1998). A thick Paleozoic succession passing from early Ordovician to Carboniferous covers the metamorphic basement associations (Yılmaz et al., 1997; Yiğitbaş et al., 1999).

Field and petrographic characteristics, obtained from the Sünnice Group suggest that the pre-early Ordovician metamorphic massifs of the IZU (namely, Sünnice, Almacık, and Armutlu) can be differentiated into four tectonostratigraphic mappable units: (1) The Çele metaophiolite, (2) the Yellice metavolcanics, (3) the Demirci metamorphics, and (4) Dirgine granite (Yiğitbaş et al., 1999). The Demirci metamorphics, which represent high-grade metamorphic ancient continental crust of the Northwestern Anatolia (Yiğitbaş and Elmas, 1997) and Dirgine granite are not discussed at any length above, therefore they are beyond the scope of this paper.

Amphibolites and basalts from the Sünnice area, the amphibolite and andesite from Armutlu, and the Almacık amphibolite all have compositional features in keeping with an intraoceanic convergent margin arc. Given the presence of ultramafic units, we interpret these rocks collectively to represent a suprasubduction ophiolite. In contrast, the Armutlu basalts have compositions consistent with a back-arc basalts, or back arc MORB-type basalts. The most straightforward interpretation is that together they represent a paired arc and back arc that were obducted together. Given the presence of arc amphibolite and andesite with the Armutlu back arc basalts, there was tectonic interleaving.

Collectively the field and geochemical data indicate that a suprasubduction ophiolite (Çele metaophiolite), an island arc (Sünnice-type mafic volcanic rocks), and a back-arc suite (Armutlu-type mafic volcanic rocks) were tectonically accreted to continental crust during the Proterozoic. This interpretation differs from earlier proposals which regard the metavolcanics as an Andean-type continental margin volcanic association built upon an ancient continental basement (Cerit, 1990; Ustaömer, 1999; Ustaömer and Rogers, 1999).

Accretion and obduction at convergent margins inevitably disrupts original stratigraphic relationships of ophiolites. Tectonic collages of ultramafic, gabbro, amphibolite and mafic volcanic units, located along, or proximal to, tectonic terrane boundaries are present in the following Precambrian areas: (1) Kibaran belt of central-southern Africa (Johnson and Oliver, 2000), (2) Superior Province of Canada (Polat and Kerrich, 2001b and reference therein), (3) Nubian shield, northeast Africa (Zimmer et al., 1995; Reischmann, 2000 and reference therein), (4) Polar Urals–Russia (Scarrow et al., 2001). In these areas, the extent of tectonic disruption varies, and most or all of the units are present. For all examples, the metamorphic grade decreases from ultramafic, through gabbro, to mafic flows, as in Phanerozoic ophiolites. The conjunction of these features has been interpreted in terms of partially and locally disrupted ophiolite sequences (Anonymous, 1972; Johnson and Oliver, 2000). The Çele metaophiolite and related volcanics have a similar conjuction of characteristics, and in keeping with the other cited examples we tentatively interpret it as an ophiolite.

Ophiolitic and volcanic associations with similar features have been described from the pre-Variscan basement of Europe along the Trans-European suture zone of Winchester (2000), or the South European suture zone of Haydoutov (1995), as well as in the Carpathians, Balkanides and Hellenides (Fig. 1 and Table 3). Some dismembered ophiolitic and island arc complexes of Precambrian or end Proterozoic–beginning Paleozoic age have also been described from the Eastern Alps and Bohemian massif (Neubauer et al., 1989; Vavra and Frisch, 1989; Bowes and Aftalion, 1991). Within the Austro-Alpine belt metamorphic basement of possibly Proterozoic age is an imbricated metamorphosed ophiolitic sequence with MORB character, an island arc volcanic suite and a back arc volcanic association (Neubauer, 1985; Haydoutov, 1995 and reference therein). In the Bohemian massif, rocks of the same age are described by Jelinek et al. (1984); Kastl and Tonika (1984) and Fiala (1977). Precambrian ophiolites and Cambrian island arc associations crop out also in the South Carpathian–Balkan region (Haydoutov, 1989). The Rhodope ophiolitic association within the metamorphic basement of the Rhodope massif occurs as oceanic crustal fragments emplaced onto an ancient continental crust (Prarhodopian Supergroup) are detailed by Kozhoukharova (1996, 1998).

When these units are considered together, they seem to belong to the South European suture zone occuring as intermittent components of a chain which is assumed to form a link between the Avalonian–Cadomian and the Arabian–Pan-African orogens (Haydoutov, 1995). Although precise ages of these complexes are not known, their stratigraphic relations and structural positions appear similar to that of the Sünnice Group. If this interpretation is valid, then the Sünnice Group forms a new addition to the intermittent chain of the late Proterozoic peri-Gondwanaland ophiolites and the South European suture.

Acknowledgements

This paper includes results of a 7 years field study supported by the TPAO (Turkish Petroleum Company) and TUBITAK grant (Turkish Scientific and Technical Research Unit; Project no. 199Y065). We thank Prof. Dr. Boris Natalin and Aral Okay for fruitful discussions on many aspects of the Pontide geology and Dr. Ali Polat for geochemistry. R. Kerrich acknowledges an NSERC Research Grant, an NSERC MFA grant, and the George McLeod endowment to the Department of Geological Sciences, University of Saskatchewan. We thank Karen McMullan for refining the text and figures. A.H.F. Robertson and J.A. Winchester critically reviewed the paper, offering many valuable suggestions which helped to improve the quality of the paper significantly.

Appendix A

Data repository 1. Major and trace element compositions of magmatic rocks of the Sunnice Area

	Ultramafic rocks			Amphibolite						Mafic volcanic rocks				Intermediate and felsic volcanic rocks			
	EY201	EY201-A	EY202	EY100	EY94	EY98	EY458	EY460	EY205	EY1-A	EY1-B	EY4	EY3	EY93	EY463	EY7	EY5
SiO_2	50.63	50.26	41.72	47.73	49.03	47.97	46.33	47.92	50.88	53.15	53.31	55.88	54.22	61.04	65.03	77.05	78.06
TiO_2	0.144	0.155	0.034	0.907	0.456	1.864	1.222	2.971	0.720	1.517	1.470	1.108	1.276	0.515	0.946	0.284	0.175
Al_2O_3	7.72	8.41	1.98	15.81	17.45	15.95	14.21	13.47	14.45	19.99	19.39	15.40	14.93	16.47	12.21	11.11	11.54
Fe_2O_3	8.6	8.0	15.4	10.8	10.4	11.4	14.2	14.5	15.7	12.6	13.2	11.7	14.3	15.5	11.8	4.2	3.7
MnO	0.135	0.123	0.171	0.172	0.166	0.196	0.184	0.267	0.283	0.199	0.190	0.226	0.270	0.340	0.244	0.071	0.081
MgO	24.0	23.1	39.8	11.0	10.3	8.9	10.5	6.7	6.6	5.2	5.4	4.1	4.8	2.1	4.1	3.4	1.3
CaO	7.70	8.77	0.91	11.35	9.53	9.57	10.94	9.80	7.78	0.63	0.66	5.63	5.61	0.58	1.74	0.31	0.16
K_2O	0.10	0.09	0.04	0.56	0.79	1.18	1.25	1.09	0.38	0.41	0.48	0.15	0.15	3.12	0.09	0.50	0.23
Na_2O	1.01	1.10	0.00	1.55	1.84	2.68	1.04	2.87	2.88	6.08	5.66	5.61	4.22	0.20	3.64	3.04	4.74
P_2O_5				0.030	0.042	0.309	0.072	0.360	0.325	0.303	0.306	0.140	0.228	0.103	0.142	0.041	0.010
LOI	1.16	1.37	14.52	1.01	3.90	1.73	1.63	1.11	3.04	3.84	4.06	5.66	3.47	3.25	2.04	2.09	1.01
Mg#	86	86	85	69	69	63	62	51	48	48	47	44	42	23	44	64	44
Cr	2,242	2,471	2,996							9	11		8				
Co	60	54	158							1	15		29				
Ni	712	689	2,077							19	1		17				
Rb	0.52	0.40	0.04	18	27	21	36	30	9	6	5	1	2	77	1	9	2
Sr	58	68	10	200	202	263	277	182	188	32	32	43	155	23	59	18	25
Ba	6	8	6	190	266	267	870	184	56	217	230	21	77	900	29	242	106
Sc	11	12	8	46	45	40	45	49	73	38	39	38	37	23	24	12	10
V	92	113	27	264	232	222	496	471	441	135	148	295	150	123	377	29	7
Ta				0.02	0.02	0.11	0.05	0.28	0.02	0.17	0.19	0.13	0.23	0.12	0.18	0.10	0.27
Nb	0.096	0.130	0.059	0.263	0.249	1.709	0.945	4.207	0.423	3.654	4.106	2.165	4.100	2.519	2.884	1.957	4.709
Zr	4.7	4.2	1.1	12	8.5	28	17	62	12	89	116	68	101	65	66	71	207
Hf	0.523	0.146	0.024	0.354	0.249	0.590	0.640	1.689	0.443	2.748	4.828	2.158	2.897	1.755	1.796	3.683	7.753
Th	0.088	0.044	0.035	0.163	0.079	0.644	0.410	1.311	0.208	1.985	2.607	1.535	1.869	3.105	2.013	2.066	2.719
U	0.021	0.023	0.018	0.062	0.026	0.296	0.307	0.359	0.072	0.557	0.589	0.496	0.502	0.789	0.292	0.414	0.893
Y	1.72	2.29	0.13	9.85	6.13	33.0	11.9	57.4	21.9	53.1	44.6	31.6	44.2	14.3	36.7	14.9	25.1
La	0.702	0.572	0.090	1.869	1.001	12.16	3.615	15.78	3.214	21.90	21.11	6.668	10.85	8.279	6.666	4.819	6.904
Ce	1.127	1.307	0.165	3.912	2.382	31.397	8.292	41.33	8.633	44.56	44.18	16.84	26.91	16.37	15.73	12.05	23.37
Pr	0.134	0.155	0.025	0.695	0.388	4.266	1.295	6.124	1.374	7.363	6.780	2.470	3.878	1.952	2.686	1.700	2.656
Nd	0.568	0.752	0.065	3.789	2.167	19.49	6.871	29.78	7.099	34.81	32.38	12.07	18.86	8.250	12.89	7.141	12.18
Sm	0.191	0.310	0.016	1.275	0.742	4.978	2.050	8.490	2.442	10.07	9.517	3.926	5.519	2.181	4.122	2.208	3.473
Eu	0.334	0.432		0.718	0.291	1.899	0.754	2.716	0.833	2.411	2.115	1.296	1.670	0.709	1.101	0.292	0.642
Gd	0.260	0.361	0.017	1.824	0.948	5.802	2.417	10.26	3.373	11.69	10.35	4.849	6.622	2.423	5.079	2.190	3.940
Tb	0.051	0.061	0.002	0.315	0.167	0.946	0.357	1.735	0.582	1.849	1.784	0.857	1.148	0.403	0.957	0.362	0.671
Dy	0.348	0.407	0.026	2.012	1.128	6.217	2.442	11.15	3.956	11.50	11.04	5.663	7.769	2.768	6.592	2.408	4.615
Ho	0.071	0.087	0.002	0.416	0.247	1.279	0.486	2.282	0.847	2.151	1.937	1.228	1.643	0.604	1.490	0.578	1.041
Er	0.185	0.246	0.020	1.122	0.658	3.511	1.332	6.469	2.520	4.754	4.462	3.552	4.631	1.746	4.372	1.821	3.280
Tm	0.027	0.035	0.006	0.147	0.099	0.505	0.181	0.932	0.363	0.705	0.580	0.516	0.693	0.259	0.653	0.268	0.524
Yb	0.193	0.245	0.015	1.023	0.658	3.276	1.120	5.766	2.383	3.827	3.687	3.453	4.498	1.759	4.505	1.972	4.136
Lu	0.024	0.033		0.136	0.085	0.472	0.162	0.790	0.353	0.514	0.479	0.496	0.657	0.263	0.587	0.308	0.629

Appendix A (*Continued*)

	Ultramafic rocks			Amphibolite						Mafic volcanic rocks				Intermediate and felsic volcanic rocks			
	EY201	EY201-A	EY202	EY100	EY94	EY98	EY458	EY460	EY205	EY1-A	EY1-B	EY4	EY3	EY93	EY463	EY7	EY5
$(La/Yb)_{cn}$	2.61	1.67	4.22	1.31	1.09	2.66	2.31	1.96	0.97	4.10	4.10	1.38	1.73	3.37	1.06	1.75	1.20
$(La/Sm)_{cn}$	2.38	1.19	3.66	0.95	0.87	1.58	1.14	1.20	0.85	1.40	1.43	1.10	1.27	2.45	1.04	1.41	1.28
$(Gd/Yb)_{cn}$	1.12	1.22	0.91	1.47	1.19	1.46	1.79	1.47	1.17	2.53	2.32	1.16	1.22	1.14	0.93	0.92	0.79
$(Eu/Eu^*)_{cn}$	4.58	3.93	0.00	1.44	1.06	1.08	1.03	0.89	0.89	0.68	0.65	0.91	0.84	0.94	0.74	0.40	0.53
Al_2O_3/TiO_2	54	54	58	17	38	9	12	5	20	13	13	14	12	32	13	39	66
Zr/Hf	9	29	47	34	34	47	26	37	27	32	24	31	35	37	36	19	27
La/Nb	7.3	4.4	1.5	7.1	4.0	7.1	3.8	3.8	7.6	6.0	5.1	3.1	2.6	3.3	2.3	2.5	1.5
Th/Nb	0.91	0.34	0.60	0.62	0.32	0.38	0.43	0.31	0.49	0.54	0.63	0.71	0.46	1.23	0.70	1.06	0.58
Th/La	0.12	0.08	0.39	0.09	0.08	0.05	0.11	0.08	0.06	0.09	0.12	0.23	0.17	0.38	0.30	0.43	0.39
Zr/Y	2.7	1.8	8.9	1.2	1.4	0.8	1.4	1.1	0.5	1.7	2.6	2.1	2.3	4.6	1.8	4.8	8.3
Zr/Nb	48.9	32.5	19.2	45.9	34.0	16.1	17.7	14.9	28.4	24.4	28.3	31.2	24.6	25.9	22.7	36.3	44.0
Ti/Zr	179	218	171	449	323	401	435	280	354	101	75	97	76	47	87	24	5
Ti/Sm	4,388	2,957	12,171	4,249	3,684	2,219	3,550	2,063	1,741	896	915	1,661	1,383	1,418	1,380	773	302
P/Nd				17.4	41.9	34.2	22.6	25.9	98.2	18.9	20.3	24.9	26.3	27.3	24.2	12.5	1.8
Ti/V	9	8	7	21	12	50	15	37	10	67	59	22	51	25	15	59	157
Sc/Lu	464	369		334	523	84	277	61	208	74	81	78	57	86	41	38	16
Nb/Nb^*	0.08	0.19	0.45	0.11	0.22	0.14	0.22	0.26	0.13	0.13	0.15	0.31	0.35	0.22	0.38	0.38	0.86
Zr/Zr^*	0.99	0.60	2.43	0.38	0.46	0.19	0.31	0.27	0.20	0.33	0.46	0.68	0.68	1.1	0.62	1.2	2.2
Hf/Hf^*	4.0	0.76	1.9	0.40	0.49	0.15	0.43	0.27	0.27	0.37	0.69	0.79	0.71	1.0	0.62	2.3	3.0
Ti/Ti^*	1.5	1.1	4.7	1.4	1.3	0.81	1.3	0.74	0.59	0.33	0.35	0.59	0.50	0.53	0.49	0.31	0.11
Sc/Y	6.5	5.4	59.7	4.6	7.3	1.2	3.8	0.85	3.35	0.71	0.87	1.2	0.84	1.6	0.65	0.78	0.39
Ce/Yb	5.85	5.33	10.8	3.82	3.62	9.58	7.41	7.17	3.62	11.6	12.0	4.88	5.98	9.31	3.49	6.11	5.65
Zr/Rb	9.04	10.6	25.2	0.67	0.32	1.33	0.47	2.10	1.36	15.8	23.1	65.6	41.8	0.84	46.4	7.81	85.6
Th/Ce	0.08	0.03	0.21	0.04	0.03	0.02	0.05	0.03	0.02	0.04	0.06	0.09	0.07	0.19	0.13	0.17	0.12
Nb/Ta				13.0	12.0	15.3	18.6	14.9	20.5	21.0	21.3	17.0	17.7	20.3	16.0	19.5	17.4

Data repository 2. Major and trace element compositions of magmatic rocks of the Almacık and Armutlu areas

	Almacık area					Armutlu area							
	Amphibolite	Intermediate and felsic volcanic rocks				Amphibolite	Mafic volcanic rocks						Intermediate volcanics
	EY12	EY8-A	EY11	EY9	EY10	EY14	EY22	EY21	EY18	EY17	EY16	EY20	EY15
SiO_2	49.31	64.99	68.85	69.28	77.09	51.35	51.01	49.94	49.07	50.09	50.00	50.39	58.42
TiO_2	0.732	0.787	0.496	0.869	0.305	0.600	1.552	1.579	1.528	1.468	1.488	1.769	0.678
Al_2O_3	16.23	14.74	13.58	12.90	11.92	16.13	15.35	15.73	15.30	15.17	15.57	14.70	15.60
Fe_2O_3	11.5	7.9	6.6	7.0	2.8	11.5	10.1	10.3	10.7	10.4	11.3	11.7	9.7
MnO	0.204	0.256	0.257	0.244	0.207	0.216	0.156	0.159	0.173	0.177	0.195	0.178	0.157
MgO	8.8	2.3	2.1	2.4	0.6	6.9	7.8	7.7	7.7	7.5	7.2	7.0	4.2
CaO	10.11	3.81	2.26	3.57	2.12	9.74	10.34	10.84	12.04	11.33	10.09	11.13	8.43
K_2O	0.18	2.46	1.64	0.53	1.71	0.59	0.20	0.26	0.39	0.19	0.15	0.08	0.12
Na_2O	2.83	2.57	4.14	2.98	3.25	2.97	3.44	3.39	2.94	3.59	3.91	2.94	2.56
P_2O_5	0.061	0.154	0.082	0.223	0.041	0.031	0.145	0.149	0.143	0.135	0.154	0.157	0.073
LOI	1.37	1.21	1.06	1.63	1.78	1.16	3.68	4.39	2.14	1.89	2.62	2.62	3.47
Mg#	63	39	41	43	32	57	63	62	61	61	58	57	49
Cr							239	244	261	222	212	127	
Co							31	36	56	34	9	16	
Ni							55	87	67	80	78	64	
Rb	1	93	31	12	40	15	5	4	8	3	3	1	2
Sr	100	125	122	350	97	150	165	170	305	186	103	280	497
Ba	46	825	391	177	451	92	17	15	33	16	17	9	33
Sc	38	24	25	21	10	57	48	47	49	48	48	47	40
V	267	94	66	27	23	320	311	324	324	319	307	347	346
Ta	0.03	0.32	0.16	0.08	0.33	0.05	0.07	0.07	0.29	0.28	0.27	0.26	0.05
Nb	0.598	5.618	3.084	1.656	5.955	1.366	1.047	1.546	4.687	4.468	4.313	4.019	0.932
Zr	20.9	86.5	57.8	91.8	114.2	11.9	47.3	89.0	94.2	96.8	92.8	77.2	19.1
Hf	0.629	2.197	1.739	2.947	3.587	0.577	1.058	1.640	2.516	2.468	3.298	2.262	0.549
Th	0.750	4.859	1.788	4.058	5.105	0.324	0.322	0.291	0.282	0.252	0.536	0.253	1.386
U	0.158	1.192	0.519	0.902	1.402	0.104	0.184	0.199	0.116	0.106	0.097	0.095	0.239
Y	13.7	25.3	27.3	44.3	28.8	22.1	30.4	30.1	28.5	27.1	27.3	33.6	14.0
La	4.935	18.56	8.734	19.69	15.12	3.501	4.833	5.113	5.139	4.857	4.875	5.250	3.917
Ce	10.42	37.76	19.82	42.82	36.16	10.31	14.26	14.35	14.74	13.81	14.07	15.23	8.973
Pr	1.462	4.596	2.647	5.594	3.900	1.613	2.315	2.262	2.386	2.110	2.216	2.486	1.244
Nd	7.022	18.48	12.35	24.94	15.77	8.075	12.07	11.66	12.12	10.47	11.19	13.56	5.464
Sm	1.924	4.270	3.492	6.689	4.136	2.456	3.794	3.803	3.676	3.454	3.565	4.234	1.534
Eu	0.684	1.201	1.146	2.076	0.775	0.728	1.330	1.346	1.377	1.275	1.237	1.549	0.561
Gd	2.244	4.726	4.259	7.431	4.685	3.060	4.758	4.753	4.650	4.373	4.519	5.547	1.960
Tb	0.386	0.728	0.750	1.227	0.791	0.548	0.869	0.837	0.803	0.733	0.774	0.965	0.324
Dy	2.568	4.916	4.987	8.475	5.147	3.638	5.553	5.570	5.243	4.812	5.267	6.524	2.137
Ho	0.531	1.012	1.061	1.743	1.101	0.830	1.184	1.123	1.044	1.041	1.085	1.332	0.460
Er	1.436	2.776	3.226	4.742	3.380	2.454	3.211	3.172	2.903	2.862	2.928	3.657	1.358
Tm	0.205	0.418	0.492	0.694	0.521	0.374	0.448	0.426	0.420	0.427	0.427	0.516	0.202
Yb	1.283	2.667	3.305	4.450	3.486	2.653	2.834	2.807	2.796	2.554	2.820	3.155	1.330
Lu	0.184	0.359	0.474	0.582	0.521	0.379	0.353	0.343	0.382	0.366	0.384	0.430	0.203

Appendix A (*Continued*)

	Almacık area					Armutlu area							
	Amphibolite	Intermediate and felsic volcanic rocks				Amphibolite	Mafic volcanic rocks						Intermediate volcanics
	EY12	EY8-A	EY11	EY9	EY10	EY14	EY22	EY21	EY18	EY17	EY16	EY20	EY15
$(La/Yb)_{cn}$	2.76	4.99	1.89	3.17	3.11	0.95	1.22	1.31	1.32	1.36	1.24	1.19	2.11
$(La/Sm)_{cn}$	1.66	2.81	1.62	1.90	2.36	0.92	0.82	0.87	0.90	0.91	0.88	0.80	1.65
$(Gd/Yb)_{cn}$	1.45	1.47	1.07	1.38	1.11	0.95	1.39	1.40	1.38	1.42	1.33	1.45	1.22
$(Eu/Eu^{*})_{cn}$	1.00	0.81	0.91	0.90	0.54	0.81	0.96	0.97	1.02	1.00	0.94	0.98	0.99
Al_2O_3/TiO_2	22	19	27	15	39	27	10	10	10	10	10	8	23
Zr/Hf	33	39	33	31	32	21	45	54	37	39	28	34	35
La/Nb	8.3	3.3	2.8	12	2.5	2.6	4.6	3.3	1.1	1.1	1.1	1.3	4.2
Th/Nb	1.25	0.86	0.58	2.45	0.86	0.24	0.31	0.19	0.06	0.06	0.12	0.06	1.49
Th/La	0.15	0.26	0.20	0.21	0.34	0.09	0.07	0.06	0.05	0.05	0.11	0.05	0.35
Zr/Y	1.5	3.4	2.1	2.1	4.0	0.5	1.6	3.0	3.3	3.6	3.4	2.3	1.4
	34.9	15.4	18.8	55.4	19.2	8.7	45.2	57.6	20.1	21.7	21.5	19.2	20.5
Ti/Zr	209	54	50	57	16	298	197	105	97	89	96	134	211
Ti/Sm	2,265	1,093	836	779	434	1,442	2,452	2,447	2,495	2,499	2,505	2,449	2,621
P/Nd	18.9	17.9	14.3	19.6	5.6	8.2	26.2	27.4	25.7	27.6	30.0	24.8	28.9
Ti/V	16	49	45	191	79	11	30	29	28	27	29	30	12
Sc/Lu	205	68	53	36	20	151	135	136	129	131	124	110	196
Nb/Nb^{*}	0.10	0.23	0.30	0.07	0.35	0.43	0.24	0.32	0.98	0.98	0.95	0.83	0.20
Zr/Zr^{*}	0.39	0.67	0.61	0.49	0.98	0.18	0.48	0.92	0.98	1.1	1.0	0.71	0.46
Hf/Hf^{*}	0.43	0.62	0.66	0.57	1.1	0.32	0.39	0.62	0.95	1.0	1.3	0.75	0.48
Ti/Ti^{*}	0.83	0.41	0.30	0.29	0.16	0.51	0.87	0.87	0.88	0.88	0.88	0.85	0.92
Sc/Y	2.8	0.97	0.92	0.47	0.36	2.6	1.6	1.5	1.7	1.8	1.7	1.4	2.9
Ce/Yb	8.12	14.16	6.00	9.62	10.37	3.89	5.03	5.11	5.27	5.41	4.99	4.83	6.75
Zr/Rb	17.1	0.93	1.90	7.43	2.88	0.78	10.4	20.8	11.6	30.3	27.6	104	8.42
Th/Ce	0.07	0.13	0.09	0.09	0.14	0.03	0.02	0.02	0.02	0.02	0.04	0.02	0.15
Nb/Ta	19.7	17.3	18.9	20.4	18.1	27.0	14.4	21.1	16.1	16.1	15.8	15.3	18.0

References

Abdüsselamoğlu, M.S., 1959. Almacıkdağı ile Mudurnu ve Göynük civarının jeolojisi. İstanbul Üniversitesi Fen Fakültesi Monografileri (Tabii İlimler Kısmı), 14, 94 pp. (in Turkish with English abstract).

Akartuna, M., 1968. Armutlu yarımadasının Jeolojisi. İstanbul Üniversitesi Fen Fakültesi Monografileri (Tabii İlimler Kısmı), 20, 105 pp. (in Turkish with French abstract).

Anonymous, 1972. Penrose conference on ophiolites. Geotimes, 17, 25.

Arpat, E., Tütüncü, K., Uysal, S., Göğer, E., 1978. Safranbolu alanında Kambriyen–Devoniyen istifi. Türkiye Jeoloji Kurumu 32. Bilimsel ve Teknik Kurultayı, Bildiri Özetleri Kitabı, 67–68 (in Turkish).

Aydın, M., Şahintürk, Ö., Serdar, H.S.S., Özçelik, Y., Akarsu, İ., Üngör, A., Çokugraş, R., Kasar, S., 1985. Çamdağ (Sakarya)–Sünnice dagı (Bolu) yöresinin jeolojisi. Türkiye Jeoloji Kurumu Bülteni 30, 1–14 (in Turkish with English abstract).

Bailey, J.C., 1981. Geochemical criteria for tectonic discrimination of orogenic andesites. Chem. Geol. 32, 139–154.

Bowes, D.R., Aftalion, M., 1991. U–Pb zircon isotopic evidence for early Ordovician and late Proterozoic units in the Marianske Lazne complex, central European Hercynides. Neues Jahrbuch fur Mineralogie-Monatshefte 7, 315–326.

Boztuğ, D., 1992. Petrography of the magmatites–metamorphites and the major element geochemistry of the magmatites in the Küre region, N Kastamonu, Central-Western Pontides. Bulletin of the Faculty of Engineering Cumhuriyet University, Serie A. Earth Sci. 9 (1), 75–106.

Campbell, I.H., Lesher, C.M., Coad, P., Franklin, J.M., Gorton, M.P., Thurston, P.C., 1984. Rare-earth element mobility in alteration pipes below massive Cu–Zn suffide deposits. Chem. Geol. 45, 181–202.

Chen, F., Siebel, W., Satır, M., Terzioğlu, M.N., 2002. Geochronology of the Karadere basement (NW Turkey) and implications for the geological evolution of the Istanbul zone. Int. J. Earth Sci. (Geol. Rundsch) 91 (3), 469–481.

Cerit, O., 1990. Bolu Masifinin jeolojik ve tektonik incelenmesi. Ph.D. Thesis, Hacettepe University, 217 pp. (in Turkish with English abstract).

Davidson, J.P., 1996. Deciphering mantle and crustal signatures in subduction zone magmatism. Subduction top to bottom. Geophys Monogr 96, American Geophysical Union, Washington, DC, pp. 251–262.

Dean, W.T., Martin, F., Monod, O., Demir, O., Rickards, R.B., Bultynck, P., Bozdoğan, N., 1997. Lower Paleozoic stratigraphy, Karadere–Zirze area, Central Pontides, Northern Turkey. In: Göncüoğlu, M.C., Derman, A.S. (Eds.), Early Paleozoic evolution in NW Gondwana, Proceedings, Turkish Associations of Petroleum Geologists Special Publication, 3, pp. 32–38.

Dostal, J., Strong, D.F., Jamieson, R.A., 1980. Trace element mobility in the mylonite zone within the Ophiolite Aureole, St. Anthony Complex, Newfoundland. Earth Plannet. Sci. Lett. 49, 188–192.

Drummond, M.S., Defant, M.J., Kepezhinskas, P.K., 1996. Petrogenesis of slab-derived trondhjemite–tonalite–dacite/adakite magmas. Transactions of the Royal Society of Edinburg. Earth Sci. 87, 205–215.

Eisenlohr, T., 1997. The thermal springs of the Armutlu peninsula (NW Turkey) and their relationship to geology and tectonic. In: Schindler, G., Pfister, M. (Eds.), Active Tectonics of Northwestern Anatolia—The MARMARA Poly-project, Hochschulverlag AG an der ETH, Zurih, pp. 197–228.

Elliot, T., Plank, T., Zindler, A., White, W., Bourdon, B., 1997. Element transport from slab to volcanic front at the Mariana arc. J. Geophys. Res. 102, 14991–15019.

Elmas, A., Yiğitbaş, E. 1998. Sünnice dağı (Bolu)'nın jeolojisi: Batı Pontid temel kayaları sorununun çözümüne petrotektonik bir yaklaşım. University of İstanbul, Research Fund Project, Report No. 705/260495, 76 pp. (in Turkish with English abstract).

Elmas, A., Yiğitbaş, E., 2001. Ophiolite emplacement by strike-slip tectonics between the Pontide Zone and the Sakarya Continent in Northwestern Anatolia, Turkey. Geologische Rundschau 90, 257–269.

Ewart, A., Hergt, J.M., Hawkins, J.W., 1994. Major element, trace element, and isotope (Pb, Sr, and Nd) geochemistry of site 839 basalts and basaltic andesites: implications for arc volcanism. Proc. Ocean Drilling Program, Scientific Results 135, 519–531.

Fiala, F., 1977. Proterozoicky vulkanismus Barrandienu a problematika spilitu. J. Geol. Sci. (Praha) 30, 7–247.

Floyd, P.A., Winchester, J.A., 1975. Magma type and tectonic discrimination using immobile elements. Earth Planet. Sci. Lett. 19, 211–218.

Frisch, W., Neubauer, F., 1989. Pre-Alpine terranes and tectonic zoning in the eastern Alps. Geol. Soc. Am. Bull. Spec. Publ. 230, 91–100.

Georgescu, M.D., 1997. Upper Jurassic-Cretaceous planktonik biofacies succession and the evolution of the Western Black Sea basin. In: Robinson, A.G. (Ed.), Regional and Petroleum Geology of the Black Sea and Surrounding Region, vol. 68. American Association of Petroleum Geologists, Memoir, pp. 169–182.

Gill, J.B., 1981. Orogenic Andesites and Plate Tectonics. Springer-Verlag, Berlin.

Göncüoğlu, M.C., 1997. Distribution of Lower Paleozoic rocks in the Alpine terranes of Turkey: paleogeographic constraints. In: Göncüoğlu, M.C., Derman, A.S. (Eds.), Early Paleozoic Evolution in NW Gondwana, Proceedings, Turkish Association of Petroleum Geologists Special Publication, 3, pp. 13–23.

Göncüoğlu, M.C., Erendil, M., Tekeli, O., Aksay, A., Kuşçu, I., Ürgün, B.M., 1987. Geology of the Armutlu Peninsula. Guidebook for the field excursion along western Anatolia, Turkey. Mineral Research and Exploration Institute (MTA), Ankara, pp. 1–19.

Goodwin, 1991. Precambrian Geology, the Dynamic Evolution of the Continental Crust. Academic Press, Harcourt Brace Jovanovich Publishers, London, 666 pp.

Görür, N., 1997. Cretaceous syn- to postrift sedimentation on the southern continental margin of the western Black Sea basin. In: Robinson, A.G. (Ed.), Regional and Petroleum Geology of the Black Sea and Surrounding Region, vol. 68. American Association of Petroleum Geologists, Memoir, pp. 227–240.

Görür, N., Tüysüz, O., Aykol, A., Sakınç, M., Yiğitbaş, E., Akkök, R., 1993. Cretaceous red pelagic carbonates of northern Turkey: their place in the opening history of the Black Sea. Eclogae Geologica Helvetica 86, 819–838.

Görür, N., Monod, O., Okay, A.İ., Şengör, A.M.C., Tüysüz, O., Yiğitbaş, E., Sakınç, M., Akkök, R., 1997. Paleogeographic and tectonic position of the Carboniferous rocks of the western Pontides (Turkey) in the frame of the Variscan belt. Bulletin de la Société Géologique de France 168 (2), 197–205.

Hawkesworth, C.J., O'Nions, R.K., Pankhurst, R.J., Hamilton, P.J., Evensen, N.M., 1977. A geochemical study of island arc and back-arc tholeiites from the Scotia Sea. Earth Planet. Sci. Lett. 36, 253–262.

Hawkesworth, C.J., Gallagher, K., Hergt, J.M., Mc Dermott, F., 1993. Mantle and slab contributions in arc magmas. Annu. Rev. Earth Planet. Sci. 21, 175–204.

Haydoutov, I., 1989. Precambrian ophiolites, Cambrian island arc, and Variscan suture in the South Carpathian–Balkan region. Geology 17, 905–908.

Haydoutov, I., 1995. Pan-African sutures along the South European suture zone. In: Erler, A. et al. (Eds.), Geology of the Black Sea Region. Proceedings of the International Symposium on the Black Sea Region, General Directorate of Mineral Research and Exploration, Ankara, pp. 3–10.

Hollings, P., Kerrich, R., 2000. An Archean arc basalt-Nb-enriched basalt-adakite association: the 2.7 Ga Confederation assemblage of the Birch-Uchi greenstone belt, Superior province. Contrib. Mineral. Petrol. 139, 208–226.

Humphris, S.E., Thompson, G., 1978. Trace element mobility during hydrothermal alteration of oceanic basalts. Geochim. Cosmochim. Acta 42, 127–136.

Hynes, A., 1980. Carbonatization and mobility of Ti, Zr in Ascot Formation basalts, SE Qubec. Contrib. Mineral. Petrol. 75, 79–87.

Jelinek, E., Pacesova, M., Misar, Z., Martinec, P., Weiss, Z., 1984. Geochemistry of a dismembered metaophiolite complex, Letovice, Czehoslovakia: Transaction of Royal Society of Edinburg. Earth Sci. 75, 37–48.

Jenner, G.A., Longerisch, H.P., Jackson, S.E., Fryer, B.J., 1990. ICP-MS a powerful tool for high precision trace element analyses in earth sciences: evidence from analyses of selected U.S.G.S reference samples. Chem. Geol. 83, 133–148.

Johnson, S.P., Oliver, G.J.H., 2000. Mesoproterozoic oceanic subduction, island arc formation and the initiation of back-arc spreading in the Kibaran Belt of central, southern Africa: evidence from the ophiolite terrane, Chewore inliers, northern Zimbabwe. Precambrian Res. 103, 125–146.

Kastl, E., Tonika, J., 1984. The Marianske Lazne metaophiolite complex (West Bohemia). Krystalinikum 17, 59–76.

Kaya, O., 1977. Gemlik–Orhangazi alanının Paleozoyik temel yapısına yaklaşım. Yerbilimleri, Hacettepe Üniversitesi 3 (1/2), 115–118 (in Turkish with English abstract).

Kaya, O., Kozur, H., 1987. A new and different Jurassic to early Cretaceous sedimentary assemblage in northwestern Turkey (Gemlik, Bursa): implication for the pre-Jurassic to early Cretaceous tectonic evolution. Yerbilimleri, Hacettepe Üniversitesi 14, 253–268.

Kozhoukharova, E., 1996. New data for the geological position of the Precambrian ophiolitic association in the Rhodope massif. Comptes rendus de l'Academie bulgare des Sciences 49 (1) 57–60.

Kozhoukharova, E., 1998. The Precambrian Rhodope ophiolitic association. Carpathian–Balkan Geological Association XVI Congress, Abstracts, Geological Survey of Austria, 305 pp.

Lev, E., Arkady, P., 1998. Some pecularities of ocean crust activity in the Mediterranean and Middle east regions. Abstracts with programs. Geol. Soc. Am. 30 (7), 352.

Longerich, H.P., Jenner, G.A., Fryer, B.J., Jackson, S.E., 1990. Inductively coupled plasma-mass spectrometric analyses of geological samples: a critical evaluation based on case studies. Chem. Geol. 83, 105–118.

Ludden, J.N., Robert, R.D.F., Taylor, R.P., 1984. Trace element mobility in alteration zones associated with Archean gold lode deposits. Econ. Geol. 79, 1131–1141.

McCulloch, M.T., Gamble, A.J., 1991. Geochemical and geodynamical constraints on subduction zone magmatism. Earth Planet. Sci. Lett. 102 (3/4), 358–374.

Macdonald, R., Hawkesworth, C.J., Heath, E., 2000. The Lesser Antilles volcanic chain: a study in arc magmatism. Earth. Sci. Rev. 49, 1–76.

MacLean, W.H., Kranidiotis, P., 1987. Immobile elements as monitors of mass transfer in hydrothermal alteration: Phelps Dodge massive sulfide deposits, Matagami, Quebec. Econ. Geol. 82, 951–962.

McDonough, W.F., Sun, S.-S., 1995. The composition of the Earth. Chem. Geol. 120, 223–253.

Middelburg, J.J., Van der Weijden, C.H., Woittiez, J.R.W., 1988. Chemical processes affecting the mobility of major and trace elements during weathering of granitic rocks. Chem. Geol. 68, 253–273.

Morris, J.D., Leeman, W.P., Tera, F., 1990. The subducted component in island arc lavas: constraints from Be isotopes and B–Be systematics. Nature 344, 31–36.

Murphy, J.B., Hynes, A.J., 1986. Contrasting secondary mobility of Ti, P, Zr, Nb, and Y in two metabasaltic suites in the Appalachians. Can. J. Earth Sci. 23, 1138–1144.

Neubauer, F., 1985. Eine praoberordovizische transgression in der grauwackenzone (Ostalpen) und ihre Bedeutung für paläozoische geodynamik und alpidischen deckenbau: Neues Jahrbuch Der Geologie und Paläontologie, Monatshefte, pp. 46–64.

Neubauer, F., Frisch, W., Schmerold, R., Schloser, H., 1989. Metamorphosed and dismembered ophiolite suites in the basement units of the Eastern Alps. Tectonophysics 164, 49–62.

Okay, A.İ., 1989. Tectonic units and sutures in the Pontides, Northern Turkey. In: Şengör, A.M.C. (Ed.), Tectonic Evolution of the Tethyan Region. NATO ASI Series C 259, 109–116.

Okay, A.İ., Şengör, A.M.C., Görür, N., 1994. Kinematic history of the opening of the Black Sea and its effect on the surrounding regions. Geology 22, 267–270.

Okay, A.İ., Satır, M., Tuysüz, O., Akyüz, S., Chen, F., 2001. The tectonics of the Strandja Massif: Variscan and mid-Mesozoic

deformation and metamorphism in the northern Aegean. Geologische Rundschau 90, 217–233.
Pearce, J.A., Parkinson, I.J., 1993. Trace-element models for mantle melting: application to volcanic arc petrogenesis. Geol. Soc. London Spec. Publ. 76, 373–403.
Pearce, J.A., Peate, D.W., 1995. Tectonic implications of the composition of volcanic arc magmas. Annu. Rev. Earth Planet. Sci. 23, 251–285.
Pearce, J.A., Kempton, P.D., Nowell, G.M., Noble, S.R., 1999. Hf–Nd element and isotope perspective on the nature and provenance of mantle and subduction components in Western Pasific arc-basin systems. J. Petrol. 40 (11), 1579–1611.
Perfit, M.R., Gust, D.A., Bence, A.E., Arculus, R.J., Taylor, S., 1980. Chemical characteristics of island-arc basalts: implications for mantle sources. Chem. Geol. 30, 227–256.
Polat, A., Kerrich, R., 2001a. Magnesian andesites, Nb-enriched basalts-andesites, and adakites from late Achean 2.7 Ga Wawa greenstone belts, Superior provence, Canada: implications for late Archean subduction zone petrogenetic processes. Contrib. Mineral. Petrol. 141, 36–52.
Polat, A., Kerrich, R., 2001b. Geodynamic processes, continental growth, and mantle evolution recorded in late Archean greenstone belts of the southern Superior Province, Canada. In: Rollinson, H.R., Whitehouse, M. (Eds.), Archaean Crustal Evolution. Precambrian Res. 112 (1/2) 5–25.
Polat, A., Kerrich, R., 2002. Nd-isotope systematics of approximately 2.7 Ga adakites, magnesian andesites, and arc basalts, Superior Province; evidence for shallow crustal recycling at Archean subduction zones. Earth Planet. Sci. Lett. 202 (2), 345–360.
Polat, A., Hofman, A.W., 2003. Alteration and geochemical patterns in the 3.7–3.8 Ga Isua greenstone belt, West Greenland. Precambrian Res. 126, 197–218.
Polat, A., Kerrich, R., Wyman, D.A., 1999. Geochemical diversity in oceanic komatiites and basalts from the late Archean Wawa greenstone belts, Superior Province, Canada: trace element and Nd isotope evidence for a heterogeneous mantle. Precambrian Res. 94 (3/4), 139–173.
Polat, A., Hofman, A.W., Münker, C., Regelous, M., Appel, P.W.U., 2003. Contrasting geochemical patterns in the 3.7–3.8 Ga pillow basalt cores and rims, Isua greenstone belt, Southwest Greenland: implications for postmagmatic alteration processes. Geochim. Cosmochim. 67 (3), 441–457.
Reischmann, T., 2000. Ophiolites and island arcs, in the late Proterozoic Nubian Shield. Ofioliti 25 (1), 1–13.
Sajona, F.G., Maury, R.C., Bellon, H., Cotton, J., Defant, M., 1996. High field strength element enrichment of Pliocene–Pleistocene island arc basalts, Zamboanga Peninsula, Western Mindanao (Philippines). J. Petrol. 37, 693–726.
Satır, M., Chen, S., Terzioğlu, N., Sieber, W., Saka, K., 2000. Late Proterozoic crustal accretion in northwestern Turkey: evidence from U–Pb and Pb–Pb zircon dating and Nd–Sr isotopes. IESCA—International Earth Sciences Colloquim on the Aegean Region, Abstracts, Dokuz Eylül University, Engineering Faculty, Department of Geology, Izmir, Turkey, 106 pp.
Scarrow, J.H., Pease, V., Fleutelot, C., Dushin, V., 2001. The late Neoproterozoic Enganape ophiolite, Polar Urals, Russia: an extension of the Cadomian arc? Precambrian Res. 110, 255–275.
Smith, T.E., 1992, Volcanic rocks of Early Proterozoic greenstone belts. In: Condie, K.C. (Ed.), Proterozoic Crustal Evolution, Developments in Precambrian Geology, vol. 10. Elsevier, Amsterdam, New York, Tokyo, pp. 7–54.
Şengör, A.M.C., 1984. The Cimmeride orogenic system and the tectonics of Eurasia. Geol. Soc. Am. Special Paper 195, 82 pp.
Şengör, A.M.C., 1995. The larger tectonic framework of the Zonguldak coal basin in northern Turkey: an outsiders view. In: Yalçın, M.N., Gürdal, G. (Eds.), Zonguldak Basin Research Wells-1: Kozlu-K20/G. Special Publication of TUBITAK-MAM, pp. 1–26.
Şengör, A.M.C., Yılmaz, Y., 1981. Tethyan evolution of Turkey: a plate tectonic approach. Tectonophysics 75, 181–241.
Şengör, A.M.C., Yılmaz, Y., Sungurlu, O., 1984. Tectonics of the Mediterranean Cimmerides: nature and evolution of the western termination of Paleotethys. In: Dixon, J.E., Robertson, A.H.F. (Eds.), The Geological Evolution of the Eastern Mediterranean. Geol. Soc. London Spec. Publ. 17, 77–112.
Tatsumi, Y., Hamilton, D.L., Nesbitt, R.W., 1986. Chemical characteristics of fluid phase released from a subducted lithosphere and origin of arc magmas: evidence from high-pressure experiments and natural rocks. J. Volcanol. Geotherm. Res. 29, 293–309.
Taylor, B., 1992. Rifting and the volcanic–tectonic evolution of the Izu-Bonin-Mariana arc. Proc. Ocean Drill Program Sci. Results 126, 627–651.
Taylor, S.R., Mc Lennan, S.M., 1985. The Continental Crust: Its Composition and Evolution. Blackwell, Oxford, 312 pp.
Ustaömer, P.A., 1999. Pre-Early Ordovisian Cadomian arc-type granitoids, the Bolu massif, West Pontides, northern Turkey: geochemical evidence. Int. J. Earth Sci.-Geologische Rundschau 88, 2–12.
Ustaömer, P.A., Rogers, G., 1999. The Bolu Massif: remnant of a pre-Early Ordovician active margin in the west Pontides, northern Turkey. Geol. Mag. 136 (5), 579–592.
Ustaömer, P.A., Mundil, R., Renne, P.R., Whitney, D.L., 2003. Time constraints on the tectono-magmatic evolution of the western Pontides (N Turkey): new U/Pb zircon ages. Eur. Geophys. Soc. Geophys. Res. Abstr. 5, 11717.
Ustaömer, T., Robertson, A.H.F., 1994. Late Paleozoic marginal basin and subduction–accretion: the Paleotethyan Küre complex, Central Pontides, northern Turkey. J. Geol. Soc. London 151, 291–305.
Ustaömer, T., Robertson, A.H.F., 1997. Tectonic-sedimentary evolution of the North Tethyan Margin in the Central Pontides of Northern Turkey. In: Robinson, A.G. (Ed.), Regional and Petroleum Geology of the Black Sea and Surrounding Region, vol. 68. American Association Petroleum Geologists, Memoir, pp. 255–290.
Vavra, G., Frisch, W., 1989. Pre-Variscan back-arc and island-arc magmatism in the Tauren window (Eastern Alps). Tectonophysics 169, 271–280.
Wilson, M., 1993. Geochemical signatures of oceanic and continental basalts a key to mantle dynamics? J. Geol. Soc. London 150, 977–990.

Winchester, J.A., Floyd, P.A., 1977. Geochemical discrimination of different magma series and their differentiation products using immobile elements. Chem. Geol. 20, 325–343.

Winchester, J.A. and the PACE TMR Network Team, 2000. Paleozoic amalgamation of central Europe: configuration of crustal blocks abutting Baltica along the Trans-European Suture Zone. International Earth Science Colloquium on the Aegean Region, IESCA-2000, Abstracts, Dokuz Eylül University Engineering Faculty, İzmir, Turkey, 18 pp.

Woodhead, J.D., Eggins, S.M., Gamble, J., 1993. High field strength and transition element systematics in island arc and back-arc basin basalts: evidence for multi-phase melt extraction and a depleted mantle wedge. EPSL 114, pp. 491–504.

Yiğitbaş E., Elmas, A., 1997. Bolu–Eskipazar–Devrek–Çaycuma dolayının jeolojisi. Turkish Petroleum Company, Unpublished Report, 94 pp. (in Turkish with English abstract).

Yiğitbaş, E., Yılmaz, Y., Şengör, A.M.C., 1995. Transcurrent plate boundary along the Rhodop–Pontide fragment: Northwestern Turkey, vol. 7. Terra Abstracts, Abstract supplement No. 1 to Terra Nova, EUG 8, Strasbourg, 176 pp.

Yiğitbaş, E., Elmas, A., Yılmaz, Y., 1999. Pre-Cenozoic tectonostratigraphic components of Western Pontides and their geological evolution. Geol. J. 34, 55–74.

Yılmaz, Y., Gözübol, A.M., Tüysüz, O., 1981. Geology of an area in and around the Northern Anatolian transform fault zone between Bolu and Akyazı. In: Işıkara, A.M., Vogel, A. (Eds.), Multidisciplinary Approach to Earthquake Prediction: Earthquake Prediction Research, Friedr, vol. 2. Vieweg and Sohn, Braunschweig/Wiesbaden, pp. 45–66.

Yılmaz, Y., Gürpınar, O., Genç, Ş.C., Bozcu, M., Yılmaz, K., Şeker, H., Yiğitbaş, E. Keskin, M., 1990. Armutlu yarımadası ve dolayının jeolojisi. Turkish Petroleum Company Report No. 2796, 210 pp. (in Turkish).

Yılmaz, Y., Genç, Ş.C., Yiğitbaş, E., Bozcu, M., Yılmaz, K., 1994. Geological evolution of the Late Mesozoic continental margin of nortwestern Anatolia. Tectonophysics 243, 155–171.

Yılmaz, Y., Tüysüz, O., Yiğitbaş, E., Genç, Ş.C., Şengör, A.M.C., 1997. Geology and tectonic evolution of the Pontides. In: Robinson, A.G. (Ed.), Regional and Petroleum Geology of the Black Sea and Surrounding Region, 68. American Association of Petroleum Geologists, Memoir, pp. 183–226.

Zimmer, M., Kröner, A., Jochum, K.P., Reischmann, T., Todt, W., 1995. The Gabal Gerf complex: a Precambrian N-MORB ophiolite in the Nubian shield, NE Africa. Chem. Geol. 123, 29–51.